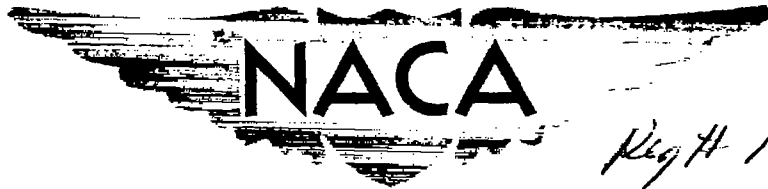


NACA RM A55L05

6473



Reg # 19738

TECH LIBRARY KAFB, NM
0143585

RESEARCH MEMORANDUM

AIRCRAFT CONFIGURATIONS DEVELOPING HIGH LIFT-DRAG
RATIOS AT HIGH SUPERSONIC SPEEDS

By A. J. Eggers, Jr., and Clarence A. Syvertson

Ames Aeronautical Laboratory
Moffett Field, Calif.

HADC
TECHNICAL LIBRARY
AFL 2811

CLASSIFIED DOCUMENT

This material contains information affecting the National Defense of the United States within the meaning of the espionage laws, Title 18, U.S.C., Secs. 793 and 794, the transmission or revelation of which in any manner to an unauthorized person is prohibited by law.

NATIONAL ADVISORY COMMITTEE
FOR AERONAUTICS

WASHINGTON

March 5, 1956

~~CONFIDENTIAL~~

SECRET

Classification

Unclassified

By Authority

NASA Tech Pub Announcement #4

By

16 Mar 59

GRADE OF OFFICER MAKING CHANGE

NK

14 Mar 61
DATE



NATIONAL ADVISORY COMMITTEE FOR AERONAUTICS

RESEARCH MEMORANDUM

AIRCRAFT CONFIGURATIONS DEVELOPING HIGH LIFT-DRAG

RATIOS AT HIGH SUPERSONIC SPEEDS

By A. J. Eggers, Jr., and Clarence A. Syvertson

SUMMARY

The problem of designing an aircraft which will develop high lift-drag ratios in flight at high supersonic speeds is attacked using the elementary principle that the components of the aircraft should be individually and collectively arranged to impart the maximum downward and the minimum forward momentum to the surrounding air. This principle in conjunction with other practical considerations of hypersonic flight leads to the study of configurations for which the body is situated entirely below the wing; that is, flat-top wing-body combinations. Theory indicates that sensibly complete aircraft of this type can be designed to develop lift-drag ratios well in excess of 6.

In order to check this possibility, several flat-top wing-body combinations consisting of a thin wing having highly swept leading and trailing edges and a half-cone body were tested at Mach numbers from 3.0 to 6.3 and Reynolds numbers (based on body length) from 5.6 to 1.1 millions. The wings were mounted flush with the upper surface of the body, the apex of each wing coinciding with the vertex of the body and the trailing edge at the root coinciding with the base of the body. The wing tips were deflected downward, thereby simulating vertical fins. Maximum lift-drag ratios of the order of 6 and greater were common to these configurations and, with one arrangement, a ratio in excess of 6.6 was obtained at the design Mach number of 5.

INTRODUCTION

Range in more or less steady level flight depends directly on aerodynamic lift-drag ratio at high supersonic speeds, just as it does at lower speeds. This result follows from the classical Breguet range equation in the case of powered flight, and it may be easily deduced from the equations of motion for unpowered or gliding flight (see refs. 1 and 2). The problem then of achieving efficient hypersonic flight is not fundamentally

new from the aerodynamic viewpoint. However, it is complicated by certain factors, some of which are new and all of which should be considered at the earliest stages in the design of a hypersonic aircraft.

Perhaps foremost among these factors is aerodynamic heating. The geometry of a hypersonic aircraft will almost certainly be governed in large part by the necessity for minimizing this phenomenon (see refs. 1 and 2). Thus, for example, the noses of bodies and leading edges of wings will tend to be round, or in some manner blunt, to reduce local heating in these regions and to provide material for absorbing heat. If the leading edge of a wing is blunt, then it appears profitable to employ sweep-back in order to reduce further the local heating and to minimize the pressure-drag penalty associated with the bluntness.¹ Finally, from the over-all point of view, it is desirable to keep the aircraft slender in order to minimize average heat-transfer rates.

Another factor which plays a leading role in hypersonic aircraft design is structural weight. With the trend toward rocket propulsion for such aircraft, very large performance gains may be obtained by reducing this weight (see, e.g., refs. 1 and 5). We are reminded, therefore, that the thin wing is basically a heavy structure by comparison to a body. In addition, the wing alone offers little advantage over the body alone in developing lift at hypersonic speeds (see ref. 1). Accordingly, there is the indication that the body should be a primary lifting element, if not the principal source of lift for a hypersonic aircraft.

The final design factor which merits attention here is that of providing stability and control in hypersonic flight. This factor can be troublesome because of the tendency of planar surfaces to lose their effectiveness (normal-force curve slope) with increasing Mach number, especially if they are located on the lee side of an aircraft (see, e.g., refs. 6, 7, and 8). The implication then is that the body should be designed to provide the maximum stabilizing influence to a hypersonic aircraft. Moreover, planar surfaces employed specifically for stability and control should, insofar as practicable, be located on the windward rather than the leeward side of the aircraft.

We have, then, a number of design factors which are dictated by considerations of aerodynamic heating, structural weight, and stability and control. These factors are, a priori, important and they should, accordingly, be kept in proper balance with those dictated by other considerations. The consideration of principal interest in this paper is range performance as it derives from lift-drag ratio. Specifically, then, the purpose of this paper is to obtain aircraft configurations which, consistent with the above-mentioned design factors, are capable of developing high lift-drag ratios at high supersonic speeds.

¹By contrast, blunting the noses of bodies need not necessarily introduce a drag penalty. Indeed, proper blunting may reduce drag (see refs. 3 and 4).

~~CONFIDENTIAL~~

NOTATION

a_o	lift-curve slope, per radian
C_D	drag coefficient, $\frac{D}{qS}$
C_L	lift coefficient, $\frac{L}{qS}$
C_m	pitching-moment coefficient, $\frac{\text{moment about body vertex}}{qSl}$
C_N	normal-force coefficient, $\frac{\text{normal force}}{qS}$
D	drag, lb
d	diameter, in.
L	lift, lb
l	length of body, in.
M	Mach number
p	static pressure, lb/sq in.
q	dynamic pressure, lb/sq in.
r	conical coordinate (measured from vertex of cone), in.
S	plan area, sq in.
x_n	distance from nose of body to neutral point, in.
α	angle of attack measured with respect to lower surface of wing, deg (radians when appearing in equations)
γ	ratio of specific heats (1.4 for air)
δ	flow deflection angle, deg
θ	flap deflection angle, deg
ω	conical ray angle, radians

~~CONFIDENTIAL~~

Subscripts

α	zero angle of attack
∞	free-stream conditions
B	body
c	evaluated at cone surface
d	design conditions
F	flap
f	friction forces
p	pressure forces
s	evaluated at shock wave
te	trailing edge
W	wing
max	maximum

THEORETICAL CONSIDERATIONS

Formulation of the Problem

At the present time there is no simple theory capable of accurately describing the flow about more or less arbitrary aircraft configurations in hypersonic flight. Accordingly, we are obliged to seek a verbal formulation of the problem which clearly defines the objective and the conditions imposed thereon.

Undertaking first to clarify the objective, we inquire how we intend to increase lift-drag ratio. A self-evident but nonetheless useful answer to this question consists of an elementary statement of requirements for efficient flight; namely, the components of an aircraft should be individually and collectively arranged to impart the maximum downward and the minimum forward momentum to the surrounding air. When these components are so arranged, we are, a priori, insured of obtaining high lift-drag ratios. Accordingly, this statement is adopted as the embodiment of our objective and, since it will be used frequently to guide our thinking, it will for convenience be referred to hereafter as simply the "momentum principle."

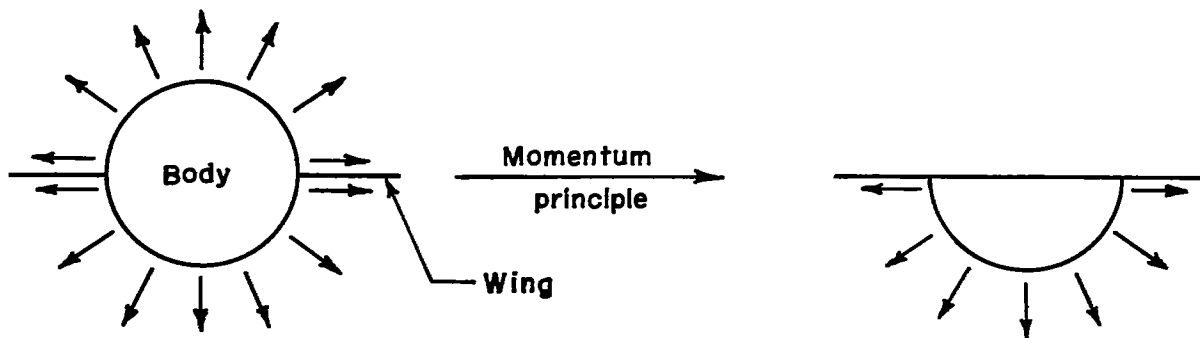
There remains the question of conditions on our objective. It was noted in the introduction that previous considerations of hypersonic

flight have suggested certain definite restrictions which may logically be imposed on the configuration of hypersonic aircraft. It is proposed to adopt these restrictions as the conditions on our objective, and they are summarized as follows: The wings of an aircraft should have highly swept, blunt leading edges, and the body should have a blunt nose. The body should, in addition, be a major lifting element, and it should be shaped to stabilize the vehicle in flight. Other stabilizing and controlling surfaces should, insofar as practicable, be located on the windward side of the aircraft. Finally, the vehicle as a whole should be of slender design.

Let us see now what manner of vehicle our attention is attracted to by the momentum principle in combination with these conditions.

General Configuration Study

It has been established that an aircraft of interest here will be slender, so we may anticipate that it will develop maximum lift-drag ratios at small angles of attack. The body should, to the extent consistent with stabilizing flight, have low pressure drag. These factors combine to draw our attention to bodies which are continuously enlarging with distance aft of the nose. They have the virtue of low drag at hypersonic speeds (see ref. 3) along with the flare effect which contributes to stability (see ref. 7). For simplicity, then, let us consider such a body of revolution mounted symmetrically on a thin wing at zero angle of attack. A front view of this arrangement, along with the disturbance velocities created by the body, is shown on the left of the sketch. Quite obviously,

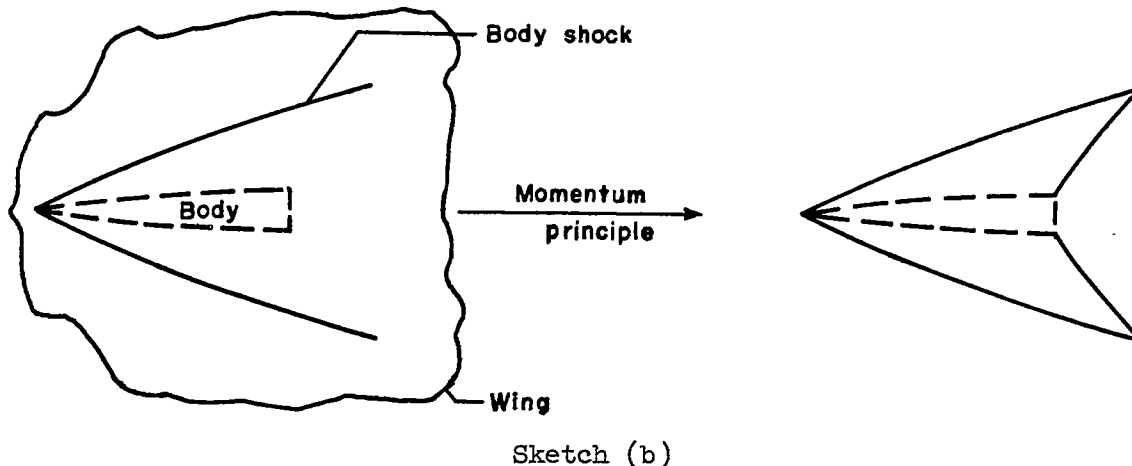


Sketch (a)

the upward momentum generated by pressure forces on the top of the body just cancels the downward momentum generated by pressure forces on the bottom of the body. According to the momentum principle and the condition that the body be a major lifting element we should, then, eliminate the upper half of the body to obtain the arrangement shown on the right of

the sketch. The wing now serves the important function of preserving the downward momentum of the air disturbed by the lower half of the body.

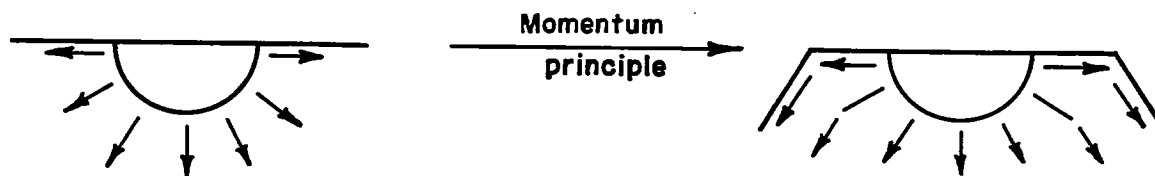
Let us consider next the plan view of this configuration shown on the left of the next sketch. The wing extends arbitrarily far beyond the body shock in this view. Now the body can impart downward momentum to the air



in the region between its surface and its shock wave. The wing, therefore, should extend out at least as far as the shock wave in order to preserve this momentum. However, any portion of the wing which extends beyond the body shock cannot serve to increase the downward momentum of the air influenced by the body. It will, however, contribute to the forward momentum imparted to the air through the action of friction forces. Thus the momentum principle suggests that the wing leading edge should coincide with the shock wave created by the body. It can similarly be reasoned that the wing should extend downstream toward, but not beyond, the line along which the body ceases to impart downward momentum to the fluid. Accordingly, it is indicated that the wing trailing edge should, like the leading edge, be swept back, and it should join with the body at its base.² We are led to suspect, then, that the configuration should appear in plan view something like the one shown at the right of sketch (b). This shape satisfies the condition of high leading-edge sweep and, too, the resulting wing tends to be of low aspect ratio which is favorable to minimizing structural weight.

²The exact trailing-edge location cannot, of course, be fixed by the elementary reasoning of this discussion, but, rather, it requires detailed study for each particular configuration with consideration, for example, of Reynolds number effects on friction forces.

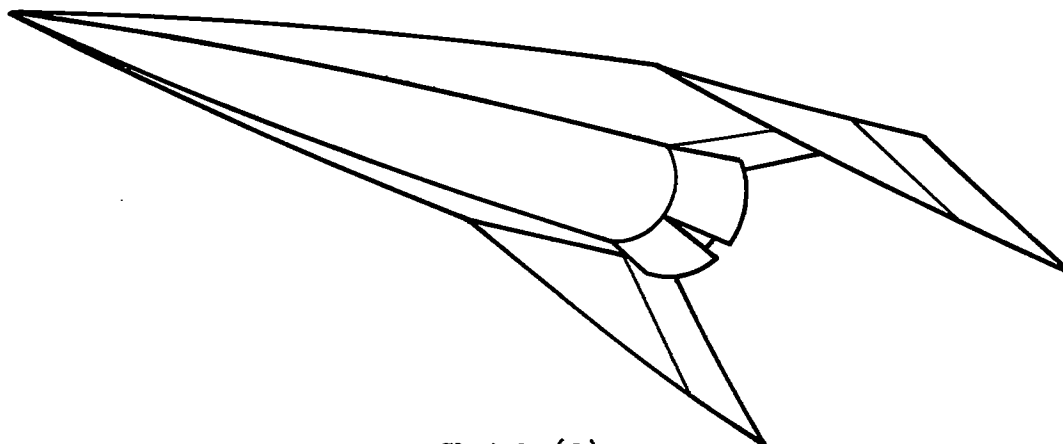
Something more may be learned, however, by again viewing the configuration from the front. Such a view is shown on the left of the next sketch. It is observed that the body imparts lateral as well as downward



Sketch (c)

momentum to the surrounding air. Now according to the momentum principle this lateral momentum should be converted into downward momentum. One way this may be accomplished without significantly increasing forward momentum is by deflecting the wing tips downward about hinge lines in the stream direction as shown on the right of sketch (c). The result is tip flaps located well aft on what would normally be the windward side of the configuration. In this location the flaps can serve two functions. One, of course, is to increase lift. Also, and perhaps more important, they are suitably located to provide directional stability and control for the configuration.

We have potentially, then, the crude semblance of a complete aircraft configuration. This point can best be appreciated by studying the schematic diagram of the vehicle shown in the next sketch. The aircraft is



Sketch (d)

of the flat-top or high-wing type with a laterally symmetric fuselage. Both wing and body contribute substantially to lift. Superficial examination suggests that the wing and body are suitably arranged to obtain stability in pitch, while control in pitch may be derived from wing trailing-edge and body flaps. The wing should, of course, contribute to damping in roll, while roll control may be obtained by differential operation of wing

flaps as ailerons. Finally, directional stability and control may be derived from the body alone, and the body and tip flaps.

The most important question is, of course, do configurations of this type actually develop high lift-drag ratios at high supersonic speeds? In order to answer this question it is necessary to examine more closely the aerodynamic characteristics of such vehicles.

Analysis of Flat-Top Wing-Body Combinations

In the following study, attention will be focused on the maximum lift-drag ratios of flat-top wing-body combinations. These combinations will be of the type just discussed, with the exception that flap effects will be neglected. These effects will be taken up later in connection with experimental results. First, then, a general class of flat-top configurations will be treated and, finally, a particular category of interest in this class will be investigated at some length.

General class of configurations.- The wings of interest here are considered to be so thin that they can be idealized as flat plates when viewed in combination with the bodies.³ The bodies of interest are one-half a body of revolution - the lower half in the view of this report. It follows that at zero angle of attack of the wing-body combination, the wing acts essentially to preserve the axial symmetry of the flow about the body. The pressure field created by the half-body forward of the trailing edge of the wing will, therefore, be the same in each meridian plane as for the corresponding whole body. It follows that the calculation of lift and drag of the combination at zero angle of attack presents no appreciable problem. The lift equals that on the body plus that on the "reflection-plane" wing. The drag equals the pressure drag of the half-body plus the friction drag of the combination.

Lift and drag of the configuration at angle of attack are more difficult to determine precisely. The simplification of axial symmetry which was exploited at $\alpha = 0$ is no longer valid and the resulting non-linear, nonisentropic hypersonic flow will require detailed examination for its accurate solution. Such an examination is far beyond the scope of this paper, however, and so we take the following very simple, but nevertheless useful, approach to the problem. It is assumed that lift varies linearly with angle of attack, while drag due to lift varies as the product of lift and angle of attack. In this event we have for the total lift and drag coefficients

³This idealization is not so impractical as it might first appear. For example, in the experiments to be discussed later, the pressure drag due to wing thickness represented only a few percent of the total drag of the test models.

~~CONFIDENTIAL~~

$$C_L = C_{L_0} + a_0 \alpha \quad (1)$$

$$C_D = C_{D_0} + C_L \alpha \quad (2)$$

Combination of equations (1) and (2) leads to the result that

$$C_D = C_{D_0} + C_{L_0} \alpha + a_0 \alpha^2 \quad (3)$$

From equations (1) and (3), the maximum lift-drag ratio at positive angles of attack is given by the relation

$$\left(\frac{L}{D}\right)_{\max} = \frac{a_0}{2 \sqrt{a_0 C_{D_0}} - C_{L_0}} \quad (4)$$

and it occurs at

$$\alpha_{(L/D)_{\max}} = \frac{\sqrt{a_0 C_{D_0}} - C_{L_0}}{a_0} \quad (5)$$

At negative angles of attack, the maximum lift-drag ratio is (in absolute value)

$$\left(-\frac{L}{D}\right)_{\max} = \frac{a_0}{2 \sqrt{a_0 C_{D_0}} + C_{L_0}} \quad (6)$$

and it occurs at

$$-\alpha_{(-L/D)_{\max}} = \frac{\sqrt{a_0 C_{D_0}} + C_{L_0}}{a_0} \quad (7)$$

Had our configurations been vertically symmetric we would, of course, have $C_{L_0} = 0$, and equation (4) for $(L/D)_{\max}$ would reduce to the familiar one

$$\left(\frac{L}{D}\right)_{\max} = \frac{a_0}{2 \sqrt{a_0 C_{D_0}}} = \frac{1}{2} \sqrt{\frac{a_0}{C_{D_0}}} \quad (8)$$

Comparison of equations (4), (6), and (8) leads to the first quantitative suggestion that flat-top configurations may develop higher than usual lift-drag ratios. Specifically, we note that the C_{L_0} term acts to increase the maximum lift-drag ratio of flat-top configurations, to decrease the ratio for flat-bottom configurations, and, of course, with

~~CONFIDENTIAL~~

symmetrical configurations there is no effect since $C_{L0} = 0$. We might anticipate then that in the order of decreasing maximum lift-drag ratio, we have the flat-top, the symmetrical, and, finally, the flat-bottom configurations of this type. In order to investigate this matter further, we are obliged to choose a particular category of shapes in the general class we have been discussing.

Particular configurations.— Certainly conical shapes are among the simplest ones to deal with. It can be argued,⁴ too, that slender shapes of this type bear a resemblance to optimum shapes (in terms of $(L/D)_{\max}$) for the conditions of given plan area and base area.⁵ Accordingly, it has been undertaken to calculate the maximum lift-drag ratios of flat-top conical configurations at high supersonic speeds. These calculations are straightforward following the approximate analysis of Appendix A in which zero base drag was assumed. They have been carried out over a range of Mach numbers using one-half a 5° (semivertex angle) cone for the body. The results are presented in figure 1. The wing was idealized as a flat plate with straight leading edges coinciding with the body shock at $\alpha = 0^\circ$. The wing trailing edges were formed by straight lines swept back from the body base and intersecting the leading edges 1.4 body lengths aft of the vertex.⁶ It is noted that the plan form changes with design Mach number.

It is not surprising that according to this figure, increasing Mach number and/or skin friction has the effect of reducing maximum lift-drag ratio. However, even with skin-friction drag coefficients as large as 0.005, the flat-top configurations tend to develop relatively high lift-drag ratios. For example, at a Mach number of 5, lift-drag ratios rather close to 7 appear to be obtainable. The maximum lift-drag ratios obtainable at negative angles of attack correspond to those of flat-bottom configurations. These ratios tend to be relatively low in absolute value. Thus, the flat-bottom configuration at a Mach number of 5 and $C_{Df} = 0.005$ has a maximum lift-drag ratio less than 5.

We have some verification, then, that properly designed wing-body combinations with flat tops have higher maximum lift-drag ratios than

⁴The argument consists simply of assuming the answer and then checking it, noting that the right circular cone is a minimum-drag body for the given conditions. The argument is considered to be somewhat qualitative, however, because it presumes that the tangent-cone approximation applies to flow between the surface and bow shock of the body in hypersonic flight $((M_\infty \delta)^2 \gg 1)$.

⁵Wing area (or plan area) is an important parameter since it couples with the weight of a vehicle to fix wing loading. Also, the base area, or more generally the maximum cross-sectional area of the body, is an important parameter since it tends (especially at hypersonic speeds) to fix the size of the cargo of a vehicle.

⁶This choice of trailing-edge location is somewhat arbitrary in relation to the present discussion. However, as will be seen, it leads to especially efficient lifting configurations in the Mach number and Reynolds number range of the experiments to be discussed later.

configurations with flat bottoms at high supersonic speeds. This finding is contradictory to previous findings which indicated according to Newtonian impact theory that flat-bottom configurations may be the more efficient (see, e.g., refs. 9 and 10). It should be noted, however, that Newtonian theory does not suggest or treat the favorable interference effects which are exploited in this paper.

Turning our attention back to equation (4), we observe that any changes in body shape which increase C_{L0} with but small increase in C_{D0} (note C_{D0} is only partly due to pressure drag) tend to bring about increases in $(L/D)_{max}$. To investigate this point more closely, calculations of $(L/D)_{max}$ have been made for wing-body combinations with various cone semivertex angles at a free-stream Mach number of 5. The results are shown in figure 2. Here again the wing leading edge was always aligned with the body shock wave and the trailing edge was formed by a straight line swept back from the base of the body and intersecting the leading edge 1.4 body lengths aft of the vertex. Several plan forms are shown in figure 2. Calculations were made for values of C_{Df} from 0 to 0.010. The results indicate that the presence of the body can be advantageous; that is, the highest $(L/D)_{max}$ is not necessarily obtained with the flat plate. At $C_{Df} = 0.005$, for example, the largest maximum lift-drag ratio is obtained with a half cone of about 5° semivertex angle mounted under the wing. Obviously, of course, if $(L/D)_{max}$ is higher for the flat-top configuration than for the flat-plate wing, then it should also be higher for the flat-top configuration than for a vertically symmetrical configuration. Just how much higher will, of course, depend upon the geometry of the symmetrical configuration.

At this point we are reminded of the approximate nature of our analysis, and a more profitable line of attack throughout the remainder of this report will be the experimental approach. Accordingly, attention is turned next to the experiments which were conducted on several flat-top configurations, with and without wing-tip flaps, and on one symmetrical configuration.

EXPERIMENT

Apparatus and Tests

Tests were conducted in the Ames 10- by 14-inch supersonic wind tunnel at Mach numbers of 3.00, 4.24, 5.05, and 6.28. For a detailed description of this wind tunnel and its aerodynamic characteristics see reference 11. Lift, drag, and pitching moment were measured with a three-component strain-gage balance. The balance system measured forces parallel and normal to the balance axis and these forces were, in turn, resolved to give the lift and drag. Pitching moments were measured about the body base, and then, through the use of the normal force, transferred to give

pitching moments about the body vertex. Tests were conducted at angles of attack from -1° to $+4^\circ$ by rotation of the model-balance assembly. All models were sting-supported from the rear where the balance was located. The support was shrouded from the air stream to within about 0.04 inch of the model base, thereby eliminating, for all practical purposes, aerodynamic loads on the sting.

Base pressures were measured in all tests and the lift and drag components of the resultant base force (referred to free-stream static pressure) were subtracted from measured total lift and drag forces to obtain the aerodynamic forces acting on the portions of the test models ahead of the base. The contribution of the base force to pitching moments was negligible.

Wind-tunnel calibration data (see ref. 11) were employed in combination with measured stagnation pressures to obtain the stream static and dynamic pressures of the tests. Reynolds numbers based on the length of the body were

<u>Mach number</u>	<u>Reynolds number, millions</u>
3.00	5.6
4.24	5.1
5.05	2.5
6.28	1.1

Models

The flat-top wing-body combinations tested in the present investigation are shown in figure 3. The body was identical for all combinations and was formed from a cone 1.250 inches in diameter, 7.144 inches in length, and having a semivertex angle of 5° . This body was chosen because of the indication (see fig. 2) that it should be a near optimum for the value of C_{Df} obtained in the 10- by 14-inch tunnel at $M_\infty = 5$. This value is, according to previous tests of other wing-body combinations, approximately 0.005. The vertex of the body was only slightly blunt with a radius of 0.002 inch.⁷ The cone was cut 1° above its axis and the wings were attached to the flat upper surface so formed. The cone was cut above the axis rather than along the axis to add depth to the body base for structural reasons.

Wings of four different plan forms were tested. These wings are referred to as plan forms A, B, C, and D, and the dimensions of each plan form are shown in figure 3. Each plan form had a semiapex angle of 12.6° .

⁷Results presented in references 3 and 4 have shown that this bluntness may be increased appreciably (e.g., to further alleviate local heating) without increasing the drag or reducing the lift of the body.

corresponding to a leading-edge sweepback of 77.4° . Under these circumstances the leading edge of the wing should essentially coincide with the shock wave generated by the body at $\alpha = 0^\circ$ and the design Mach number of 5 (see ref. 12). The four plan forms differed only in trailing-edge and tip shape. The basic configuration, plan form A, had its trailing edge swept back from the base of the body to intersect the leading edge 1.4 body lengths aft of the vertex. Calculations indicated that this particular arrangement represented a good compromise, in terms of obtaining high lift-drag ratios, between the lift and drag (especially friction drag) carried by the wing. The other plan forms were chosen simply because they represent some rather obvious variations on plan form A.

The leading edges of all wings were blunt and 0.004 inch thick. The corresponding thickness for a full-scale aircraft would be of the order of several tenths of an inch. According to estimate, this thickness should be sufficient in steady level flight at the design Mach number of 5 to keep the surface temperatures for equilibrium between convective and radiant heat transfer well below 1500°R at the leading edge (see ref. 2). All wing surfaces were flat and the bottom surface was aligned with the free stream at $\alpha = 0^\circ$. The wing sections were essentially simple wedges, 1.75 percent thick in streamwise planes and 7.83 percent thick in planes normal to the leading edge. The maximum wing thickness was 0.125 inch at the center line of the base of the body.

Plan forms A and C were tested with tip flaps formed by deflecting downward the outboard portions of the wings along streamwise hinge lines.⁸ Flap deflections of 0° , 30° , and 60° were employed. The flap hinge lines were located 1.125 inches (i.e., 50 percent of the wing semispan) from the configuration center line. With this location, approximate calculations indicated that at $M_\infty = 5$ and angles of attack up to 4° , the positive pressure field due to flap deflection would not intersect the body ahead of the base and thereby increase pressure drag.⁹ A model employing plan form A was also tested with a flap having a hinge line canted 5° . The canted hinge line intersected the wing leading edge 1.222 inches, and the trailing edge 1.015 inches outboard of the configuration center line. This flap had the same area as the one with the streamwise hinge line.

⁸Mechanically, the flaps were formed by first milling a small groove along the hinge line. The wing was then bent along this line and the groove filled and faired to mate the wing contour. This construction simulates a sealed-flap condition in the usual terminology.

⁹It was presumed that this condition would be satisfied if the Mach line emanating downstream from the intersection of the hinge line and the wing leading edge passed behind the body base. The Mach line was located by considering the flow about the body to be the same as that which exists about a 5° semivertex-angle cone operating at $\alpha = 0^\circ$ and at a free-stream Mach number equal to the Mach number on the bottom surface of a flat plate inclined 4° at $M_\infty = 5$.

In addition to these models, a model with a body consisting of a right circular cone was tested. This model had a wing identical to plan form A. The body was located symmetrically on the wing and had a semivertex angle of 4.30° and a base diameter of 1.074 inches. The resulting model had the same wing thickness, body length, body base area, wing base area, body volume, and wing volume as the flat-top configuration with plan form A.

A table giving aspect ratio, total wing area, total flap area, and the ratio of flap to wing area is presented in figure 3 for all configurations tested.

Accuracy of Test Results

In the region of the test models, stream Mach numbers did not vary by more than ± 0.02 at Mach numbers of 3.00, 4.24, and 5.05. A maximum variation of ± 0.04 existed at the peak test Mach number of 6.28. Reynolds numbers did not vary by more than $\pm 20,000$ from the values previously noted. Uncertainties in the angle of attack due to irregularities in the wind-tunnel air stream and to inaccuracies in the determination of the model support deflections are estimated to be $\pm 0.1^\circ$.

The accuracy of the test results is affected by uncertainties in the measurement of forces and moments, and in the determination of angle of attack and stream static and dynamic pressures. These uncertainties led to estimated uncertainties in the various force and moment coefficients and lift-drag ratios as shown in the following table:

M_∞	C_L	C_D	C_m	L/D
3.00	± 0.001	± 0.0002	± 0.001	± 0.2
4.24	± 0.001	± 0.0002	± 0.001	± 0.2
5.05	± 0.001	± 0.0002	± 0.001	± 0.2
6.28	± 0.002	± 0.0004	- - -	± 0.3

It should be noted that, for the most part, the experimental results presented herein are in error by less than these estimates.

In the course of the present investigation, the symmetrical model was tested upright and inverted, and to negative as well as positive angles of attack. The data obtained in all attitudes agreed within the accuracies shown in the table.

RESULTS AND DISCUSSION

All of the experimental results obtained in the present investigation are tabulated in table I. Only those portions of these data which are essential to demonstrating the main points of this paper will be presented in graphical form.

The measured lift coefficients and lift-drag ratios of basic plan form A are presented in figure 4 for various flap deflections and free-stream Mach numbers. These test results are more or less typical of those obtained with the other flat-top configurations. It is observed that plan form A is aerodynamically efficient, developing lift-drag ratios in excess of 6 at all but the highest test Mach number. Note that the maximum lift-drag ratios occur at relatively low angles of attack, ranging from 3° to 4° . The corresponding lift coefficients are, as a result, also low, ranging from 0.06 to 0.1. Configurations of this type will fly, then, at relatively high values of dynamic pressure.

It is also observed in figure 4 that the effect of deflecting the tip downward is to reduce slightly maximum lift-drag ratio. A better understanding of this result can be obtained from figure 5 where the lift and drag coefficients and lift-drag ratios of plan form A, with and without deflected wing tips, are shown as a function of angle of attack at a Mach number of 5.05. It is seen that deflecting the wing tips 60° increased the lift by as much as 50 percent with essentially no penalty in drag near $\alpha = 0$. Accordingly, the lift-drag ratios of the deflected-tip configuration are substantially increased, as was anticipated, at very small angles of attack. On the other hand, the lift-curve slope is lower and the drag is higher at positive angles of attack for the deflected tip configuration. It is these effects which cause a reduction in maximum lift-drag ratio with tip deflection about streamwise hinge lines. As might be expected, canting the hinge lines to the stream direction tends to eliminate the loss in lift-curve slope (see fig. 5); however, the drag penalty more than compensates for this improvement, with the result that $(L/D)_{\max}$ is still lower than that for the configuration with streamwise hinge lines.

The maximum lift-drag ratios of the various configurations tested are presented in figure 6 as a function of Mach number. It is seen that the highest lift-drag ratio is 6.65, and this was obtained with basic plan form A ($\theta_F = 0^\circ$) at the design Mach number of 5. Interestingly enough, this value of $(L/D)_{\max}$ compares well with the value of 6.85 predicted theoretically for ideal conical configurations of this type (see fig. 2).¹⁰ Figure 6 shows clearly the marked reduction in lift-drag ratio associated with increasing the Mach number from 5.05 to 6.28. This reduction is no

¹⁰This rather close agreement is, to be sure, due in good part to compensating errors in the approximate expressions used to calculate lift and drag and hence lift-drag ratio in this report.

doubt in part due to departing from the design conditions of the configurations; however, it is better viewed as a characteristic result of the very low test Reynolds number accompanying the highest test Mach number in the Ames 10- by 14-inch supersonic wind tunnel (see section on "Apparatus and Tests").

It is also interesting to note in figure 6 that the maximum lift-drag ratios of the flat-top model are substantially higher than those of the corresponding symmetrical configuration, especially near the design Mach number. This point is illustrated more clearly in figure 7 where the lift-drag ratios of the two models are shown as a function of lift coefficient at a Mach number of 5.05. The maximum lift-drag ratio is observed to be about 15 percent higher for the flat-top model than for the symmetrical model. According to the approximate theory of this report, about a 17-percent increase in $(L/D)_{\max}$ would be expected.

As a final point in this discussion, it is appropriate to consider briefly the pitching-moment characteristics of the various test models. To this end, pitching-moment coefficients as a function of lift coefficient are shown in figure 8 for various flap deflections on the plan form A model at Mach numbers up to 5.05.¹¹ In general, the variation of C_m with C_L is linear over the test range of lift coefficients. In figure 9 the neutral points of several of the test configurations are presented as a function of Mach number. It is apparent from figure 9(a) that the neutral point for plan form A is slightly forward for a flap deflection of 60° and close to the center of area of the wing. For all configurations the neutral point is relatively insensitive to changes in Mach number; for example, it moves aft only about 2 percent of the body length as the Mach number is increased from 3.00 to 5.05. This result is, of course, desirable from the standpoint of maintaining static longitudinal stability.

CONCLUDING REMARKS

It has been deduced with the aid of an elementary momentum principle that flat-top configurations consisting of a half body situated underneath a thin triangular wing having highly swept leading and trailing edges may be aerodynamically efficient in hypersonic flight. This possibility was verified theoretically and experimentally in the case of conical configurations of this type. For example, maximum lift-drag ratios in excess of 6.6 were obtained at a Mach number of 5 and a Reynolds number of 2.5×10^8 . These ratios were about 15 percent higher than those of an entirely comparable symmetrical configuration and, according to theory, they should exceed those of corresponding flat-bottom configurations by more like twice this percentage. Pitching-moment coefficients of the flat-top configurations were found experimentally to vary essentially linearly with lift coefficient. Neutral points were essentially constant at locations

¹¹Pitching-moment data were not obtained at $M_\infty = 6.28$.

ENDING

from 2 to 4 percent of the root chord aft of the center of plan area over the Mach number range from 3 to 5.

It was also suggested that lift-drag ratios of flat-top configurations might be increased by deflecting the wing tips downward about hinge lines in the stream direction. This possibility was borne out by experiment near zero angle of attack; however, maximum lift-drag ratios were slightly reduced. For example, they were in the neighborhood of 6 for tip deflections of 60° at a Mach number of 5. One practical interpretation of these results is, of course, that the wing tips may be employed like vertical-tail surfaces for the present flat-top configurations, with but small loss in flight efficiency.

The flat-top aircraft configuration is, then, capable of developing high lift-drag ratios at high supersonic speeds. These lift-drag ratios are, furthermore, especially susceptible to improvement by methods which reduce friction drag. (Note, e.g., that friction drag was three to four times greater than pressure drag on the test models of this paper at $M_\infty = 5$ and $\alpha = 0^\circ$.) Indeed, reducing friction drag not only benefits the basic flat-top configuration, but moreover it shifts the angle of attack for $(L/D)_{\max}$ toward zero, thereby improving the performance of tip flaps. Certainly, then, tests at higher Reynolds numbers approaching those encountered in flight appear desirable.

These are some of the possibilities which attract attention. It is important, however, to emphasize the preliminary nature of the present report. More elaborate theoretical and experimental studies are required to assess the full value of the flat-top configurations.

Ames Aeronautical Laboratory
National Advisory Committee for Aeronautics
Moffett Field, Calif., Dec. 5, 1955

APPENDIX A

APPROXIMATE CALCULATION OF MAXIMUM LIFT-DRAG RATIOS
OF FLAT-TOP CONICAL CONFIGURATIONS

Consider a thin wing mounted on top of one-half a right circular cone. The lift force exerted on the wing at zero angle of attack is obtained by integration of the conical pressure field acting on its lower surface. Thus, we may write

$$C_{L_{OW}} = \frac{2}{\gamma M_{\infty}^2 S} \int_{\omega_c}^{\omega_s} \left(\frac{p}{p_{\infty}} - 1 \right) r_{te}^2 d\omega \quad (A1)$$

where p/p_{∞} is the same function of ω as for a noninclined right circular cone (see, e.g., ref. 12), and r_{te} is the radial distance from the apex of the wing to the trailing edge. Thus r_{te} is a function of ω , depending on the plan form of the wing. The lift coefficient of the body is given by the expression

$$C_{L_{OB}} = \frac{d^2}{2\gamma M_{\infty}^2 S \tan \delta_c} \left(\frac{p_c}{p_{\infty}} - 1 \right) \quad (A2)$$

while the pressure drag coefficient of the body is (exclusive of base drag)¹

$$C_{D_{Op}} = \frac{\pi d^2}{4\gamma M_{\infty}^2 S} \left(\frac{p_c}{p_{\infty}} - 1 \right) \quad (A3)$$

The total lift and drag coefficients of the configuration at zero angle of attack are, then, to the accuracy of this analysis,

$$C_{L_O} = C_{L_{OW}} + C_{L_{OB}} \quad (A4)$$

¹The justification for neglecting base drag is that it is normally a small percentage of total drag in unpowered hypersonic flight, while in powered flight it may be positive or negative, depending upon the power-plant installation.

$$C_{D_0} = C_{D_{0p}} + C_{D_f} \quad (A5)$$

where C_{D_f} is the skin-friction drag coefficient.

The next question to be answered is: What is the lift-curve slope of the configuration? In order to accurately calculate this quantity, a careful study of the conical flow about the configuration at angle of attack will be required. Such a study is beyond the scope of this paper; accordingly, we adopt the approximate linear-theory estimate of lift-curve slope; namely,

$$\alpha_0 = \frac{4}{\sqrt{M_\infty^2 - 1}} \quad (A6)$$

which will be satisfactory for our purposes.²

Equations (A1) through (A6), in combination with equation (4), provide us with the necessary information to calculate the maximum lift-drag ratios of flat-top configurations of conical shape.

²It will not be attempted to justify equation (A6) beyond the fact that it is a rather obvious approximation for slender configurations at the small (of the order of a few degrees) angles of attack of interest here. Again it is emphasized, however, that in the opinion of the authors, the whole aspect of flat-top configurations at angle of attack will require close examination (including effects of the bow shock wave and other non-linear features of the flow) before their lifting characteristics are well understood.

REFERENCES

1. Eggers, Alfred J., Jr., Allen, H. Julian, and Neice, Stanford E.: A Comparative Analysis of the Performance of Long-Range Hypervelocity Vehicles. NACA RM A54L10, 1955.
2. Seiff, Alvin, and Allen, H. Julian: Some Aspects of the Design of Hypersonic Boost-Glide Aircraft. NACA RM A55E26, 1955.
3. Eggers, A. J., Jr., Dennis, David H., and Resnikoff, Meyer M.: Bodies of Revolution for Minimum Drag at High Supersonic Airspeeds. NACA RM A51K27, 1952.
4. Sommer, Simon C., and Stark, James A.: The Effect of Bluntness on the Drag of Spherical-Tipped Truncated Cones of Fineness Ratio 3 at Mach Numbers 1.2 to 7.4. NACA RM A52B13, 1952.
5. Allen, H. Julian, and Eggers, A. J., Jr.: A Study of the Motion and Heating of Missiles Entering the Earth's Atmosphere at High Supersonic Speeds. NACA RM A53D28, 1953.
6. McLellan, Charles H.: A Method for Increasing the Effectiveness of Stabilizing Surfaces at High Supersonic Mach Numbers. NACA RM L54F21, 1954.
7. Eggers, A. J., Jr., and Syvertson, Clarence A.: Experimental Investigation of a Body Flare for Obtaining Pitch Stability and a Body Flap for Obtaining Pitch Control in Hypersonic Flight. NACA RM A54J13, 1955.
8. Wong, Thomas J., and Gloria, Hermilo R.: Aerodynamic Characteristics of Two Rectangular Plan Form All-Movable Controls in Combination With a Slender Body of Revolution at Mach Numbers From 3.00 to 6.25. NACA RM A55J07, 1956.
9. Sanger, Eugen: Raketen-flugtechnik. R. Oldenbourg (Berlin), 1933.
10. Resnikoff, Meyer M.: Optimum Lifting Bodies at High Supersonic Speeds. NACA RM A54B15, 1954.
11. Eggers, A. J., Jr., and Nothwang, George J.: The Ames 10- by 14-Inch Supersonic Wind Tunnel. NACA TN 3095, 1954.
12. Staff of Computing Section, Massachusetts Institute of Technology, Dept. of Elect. Engr., Center of Analysis, under the direction of Zdenek Kopal: Tech. Rep. No. 1, Tables of Supersonic Flow Around Cones, Cambridge, Mass., 1947.

TABLE I.- AERODYNAMIC CHARACTERISTICS OF TEST CONFIGURATIONS

Plan form A																				
$M_\infty = 3.00$					$M_\infty = 4.04$					$M_\infty = 5.05$					$M_\infty = 6.28$					
α	C_L	C_D	L/D	C_m	α	C_L	C_D	L/D	C_m	α	C_L	C_D	L/D	C_m	α	C_L	C_D	L/D	C_m	
0	-0.79	0.0003	0.0003	0.03	0.0000	-0.88	0.0072	0.0077	-0.94	0.0088	-0.0073	0.0095	-0.0073	0.0095	0	-1.13	0.0099	0.0098	-0.10	0.0000
1	-0.30	0.0004	0.0009	1.17	-0.0077	-0.48	0.0046	0.0074	-0.61	0.0083	-0.0047	0.0079	-0.60	0.0095	1	-0.68	0.0069	0.0068	-0.76	0.0000
2	0.21	0.0006	0.0010	8.69	-0.0154	0.03	0.0156	0.0071	8.61	-0.0109	0.07	0.0131	0.0059	8.83	2	-0.11	0.0139	0.0092	1.69	0.0000
3	0.70	0.0010	0.0013	5.33	-0.0288	0.10	0.0261	0.0073	5.38	-0.0194	0.20	0.0215	0.0059	5.66	3	0.48	0.0200	0.0095	2.59	0.0000
4	1.19	0.0043	0.0098	1.58	-0.0388	0.36	0.0377	0.0079	1.53	-0.0271	1.06	0.0297	0.0065	1.78	4	0.94	0.0295	0.0088	3.37	0.0000
5	1.69	0.0098	0.0105	1.70	-0.0481	0.62	0.0472	0.0081	1.62	-0.0349	1.49	0.0328	0.0068	2.40	5	1.47	0.0371	0.0092	4.04	0.0000
6	2.17	0.0190	0.0111	1.70	-0.0509	0.89	0.0494	0.0092	1.69	-0.0422	1.97	0.0404	0.0074	2.83	6	1.99	0.0450	0.0101	4.44	0.0000
7	2.67	0.0274	0.0185	1.70	-0.0598	1.15	0.0592	0.0108	1.62	-0.0493	2.44	0.0481	0.0083	3.20	7	2.58	0.0520	0.0109	4.70	0.0000
8	3.15	0.0374	0.0198	1.70	-0.0682	1.41	0.0718	0.0113	1.56	-0.0562	2.92	0.0516	0.0093	3.61	8	3.06	0.0593	0.0118	5.05	0.0000
9	3.68	0.0499	0.0205	1.70	-0.0778	1.65	0.0820	0.0126	1.50	-0.0627	3.40	0.0628	0.0103	4.01	9	3.58	0.0670	0.0130	5.15	0.0000
10						1.85	0.0886	0.0141	1.48	-0.0691	3.88	0.0739	0.0117	4.50	10	4.10	0.0740	0.0143	5.18	0.0000
30	-0.76	0.0070	0.0098	1.73	-0.0009	-0.87	0.0080	0.0071	1.89	-0.0080	-0.88	0.0091	0.0065	1.97	30	-1.12	0.0083	0.0078	1.30	0.0000
31	-0.87	0.0170	0.0093	1.86	-0.0043	-0.88	0.0110	0.0070	1.97	-0.0094	-0.88	0.0108	0.0065	1.97	31	-0.61	0.0096	0.0078	1.88	0.0000
32	-0.86	0.0267	0.0096	2.79	-0.0019	0.03	0.0109	0.0078	2.76	-0.0105	0.09	0.0100	0.0064	2.95	32	-0.08	0.0108	0.0081	1.90	0.0000
33	-0.70	0.0071	0.0100	1.70	-0.0302	0.00	0.0071	0.0074	1.61	-0.0282	0.06	0.0074	0.0066	1.19	33	0.96	0.0080	0.0086	2.77	0.0000
34	1.19	0.0474	0.0105	1.50	-0.0305	0.25	0.0371	0.0080	1.64	-0.0308	0.73	0.0328	0.0070	2.04	34	0.97	0.0304	0.0083	3.44	0.0000
35	1.68	0.0397	0.0114	1.53	-0.0472	0.53	0.0492	0.0085	1.58	-0.0369	1.48	0.0431	0.0078	2.66	35	1.49	0.0374	0.0093	4.08	0.0000
36	2.16	0.0693	0.0133	1.63	-0.0529	0.80	0.0693	0.0094	1.90	-0.0469	2.16	0.0631	0.0083	3.03	36	2.09	0.0619	0.0103	4.80	0.0000
37	2.65	0.0877	0.0133	1.97	-0.0538	1.08	0.0877	0.0103	2.11	-0.0505	2.65	0.0808	0.0095	3.21	37	2.59	0.0804	0.0107	4.70	0.0000
38	3.14	0.0914	0.0145	2.15	-0.0519	1.36	0.0914	0.0114	2.27	-0.0471	3.14	0.0869	0.0105	3.40	38	3.08	0.0777	0.0110	4.82	0.0000
39	3.62	0.0980	0.0144	2.51	-0.0499	1.65	0.0981	0.0127	2.30	-0.0461	3.62	0.0931	0.0117	3.62	39	3.61	0.0801	0.0118	4.90	0.0000
40	4.11	0.1130	0.0183	2.24	-0.0600	1.90	0.0887	0.0148	2.44	-0.0707	4.11	0.0875	0.0128	3.88	40	4.11	0.0713	0.0145	4.93	0.0000
60	-0.77	0.0121	0.0090	1.34	-0.0118	-0.80	0.0079	0.0078	1.69	-0.0082	-0.89	0.0089	0.0068	1.08	60	-1.13	0.0048	0.0078	1.82	0.0000
61	-0.80	0.0196	0.0091	2.15	-0.0172	-0.81	0.0142	0.0078	1.68	-0.0129	-0.81	0.0138	0.0068	1.10	61	-0.62	0.0058	0.0068	1.12	0.0000
62	-0.80	0.0278	0.0094	2.97	-0.0078	-0.81	0.0219	0.0076	2.88	-0.0139	-0.81	0.0217	0.0068	1.10	62	-0.10	0.0071	0.0068	1.87	0.0000
63	-0.71	0.0094	0.0096	1.78	-0.0288	0.00	0.0094	0.0078	1.71	-0.0287	0.00	0.0094	0.0068	1.17	63	0.98	0.0044	0.0069	2.57	0.0000
64	1.19	0.0498	0.0104	1.40	-0.0361	0.00	0.0498	0.0084	1.33	-0.0288	0.00	0.0498	0.0068	1.10	64	0.94	0.0093	0.0100	3.08	0.0000
65	1.68	0.0398	0.0118	1.49	-0.0489	0.00	0.0398	0.0090	1.34	-0.0313	0.00	0.0398	0.0068	1.10	65	1.48	0.0078	0.0106	3.98	0.0000
66	2.17	0.0650	0.0121	1.76	-0.0501	0.00	0.0650	0.0098	1.59	-0.0388	0.00	0.0650	0.0068	1.10	66	2.00	0.0437	0.0116	3.78	0.0000
67	2.66	0.0799	0.0133	1.98	-0.0474	0.00	0.0799	0.0106	1.84	-0.0401	0.00	0.0799	0.0068	1.10	67	2.53	0.0505	0.0124	4.08	0.0000
68	3.15	0.0847	0.0137	2.29	-0.0486	0.00	0.0847	0.0119	2.08	-0.0314	0.00	0.0847	0.0068	1.10	68	3.02	0.0573	0.0130	4.10	0.0000
69	3.64	0.0945	0.0162	2.24	-0.0471	0.00	0.0945	0.0138	2.38	-0.0328	0.00	0.0945	0.0068	1.10	69	3.58	0.0646	0.0138	4.80	0.0000
70	4.12	0.1077	0.0179	2.29	-0.0493	0.00	0.1077	0.0146	2.68	-0.0388	0.00	0.1077	0.0068	1.10	70	4.10	0.0704	0.0168	4.18	0.0000
Plan form A (cont'd wings line)																				
15	-0.77	0.0187	0.0099	1.34	-0.0101	0.00	0.0186	0.0091	1.40	-0.0095	0.00	0.0186	0.0091	1.40	15	-1.14	0.0094	0.0091	0.37	0.0000
16	-0.89	0.0198	0.0099	1.45	-0.0108	0.00	0.0198	0.0091	1.49	-0.0094	0.00	0.0198	0.0091	1.49	16	-0.68	0.0108	0.0091	1.15	0.0000
17	-0.88	0.0284	0.0098	3.03	-0.0227	0.00	0.0284	0.0091	2.93	-0.0109	0.00	0.0284	0.0091	2.93	17	-0.11	0.0118	0.0091	1.94	0.0000
18	-0.71	0.0099	0.0103	1.88	-0.0338	0.00	0.0099	0.0091	1.88	-0.0338	0.00	0.0099	0.0091	1.88	18	0.98	0.0099	0.0091	2.68	0.0000
19	1.61	0.0494	0.0110	1.68	-0.0411	0.00	0.0494	0.0094	1.68	-0.0411	0.00	0.0494	0.0094	1.68	19	0.94	0.0134	0.0100	3.33	0.0000
20	1.70	0.0680	0.0116	1.57	-0.0313	0.00	0.0680	0.0101	1.71	-0.0313	0.00	0.0680	0.0101	1.71	20	1.48	0.0405	0.0107	3.77	0.0000
21	2.19	0.0731	0.0126	1.70	-0.0301	0.00	0.0731	0.0101	1.88	-0.0407	0.00	0.0731	0.0101	1.88	21	2.00	0.0473	0.0114	4.16	0.0000
22	2.68	0.0848	0.0138	1.94	-0.0306	0.00	0.0848	0.0101	2.00	-0.0408	0.00	0.0848	0.0101	2.00	22	2.53	0.0525	0.0124	4.46	0.0000
23	3.18	0.0921	0.0137	2.30	-0.0289	0.00	0.0921	0.0101	2.30	-0.0289	0.00	0.0921	0.0101	2.30	23	3.02	0.0604	0.0136	4.58	0.0000
24	3.67	0.1004	0.0139	2.60	-0.0273	0.00	0.1004	0.0101	2.60	-0.0273	0.00	0.1004	0.0101	2.60	24	3.51	0.0686	0.0138	4.75	0.0000
Plan form A (symmetrical model)																				
0	-0.84	0.0184	0.0096	1.94	-0.0136	0.00	-0.90	0.0190	0.0076	-0.90	0.0190	-0.0076	0.0090	0	-0.90	0.0194	0.0071	-0.93	0.0000	
1	-0.35	0.0076	0.0099	1.80	-0.0095	0.00	-0.41	0.0077	0.0073	-0.41	0.0077	-0.0073	0.0066	1	-0.43	0.0078	0.0069	-1.04	0.0000	
2	0.14	0.0068	0.0095	2.89	-0.0083	0.00	-0.01	0.0001	0.0078	-0.01	0.0001	-0.0078	0.0066	2	0.04	0.0005	0.0069	-0.0003	0.0000	
3	0.64	0.0138	0.0097	1.49	-0.0102	0.00	0.66	0.0098	0.0074	1.38	-0.0097	0.0098	0.0066	3	0.01	0.0028	0.0069	1.28	0.0000	
4	1.12	0.0245	0.0100	1.46	-0.0120	0.00	1.13	0.0196	0.0077	1.25	-0.0120	0.0197	0.0066	4	0.08	0.0079	0.0071	0.28	0.0000	
5	1.61	0.0361	0.0109	1.44	-0.0088	0.00	1.40	0.0090	0.0088	1.54	-0.0088	0.0090	0.0066	5	1.46	0.0174	0.0073	0.048	0.0000	
6	2.10	0.0478	0.0113	1.38	-0.0095	0.00	1.87	0.0136	0.0087	1.81	-0.0095	0.0136	0.0066	6	1.92	0.0244	0.0074	0.084	0.0000	
7	2.60	0.0594	0.0123	1.43	-0.0088	0.00	2.37	0.0179	0.0087	2.37	-0.0088	0.0179	0.0066	7	2.46	0.0348	0.0074	0.137	0.0000	
8	3.09	0.0705	0.0135	1.58	-0.0080	0.00	2.89	0.0259	0.0093	2.38	-0.0114	0.0259	0.0066	8	2.90	0.0468	0.0084	0.20	0.0000	
9	3.59	0.0810	0.0147	1.51	-0.0081	0.00	3.38	0.0360	0.0112	2.54	-0.0127	0.0360	0.0066	9	3.10	0.0597	0.0093	0.27	0.0000	
10	3.85	0.0870	0.0153	1.59	-0.0079	0.00	3.66	0.0410	0.0121	2.79	-0.0134	0.0410	0.0066	10	3.27	0.0701	0.0105	0.31	0.0000	

TABLE I.- AERODYNAMIC CHARACTERISTICS OF TEST CONFIGURATIONS - Concluded.

Plan form B																												
$M_\infty = 3.00$						$M_\infty = 4.84$						$M_\infty = 5.05$						$M_\infty = 6.28$										
θ , deg	α	C_L	C_D	L/D	C_M	θ , deg	α	C_L	C_D	L/D	C_M	θ , deg	α	C_L	C_D	L/D	C_M	θ , deg	α	C_L	C_D	L/D	C_M					
0	-0.76	0.0041	0.0005	0.43	---	0	-0.87	0.0008	0.0009	-0.03	---	0	-0.88	0.0015	0.0003	0.43	---	0	---	---	---	---	---					
19	0.0206	0.0087	0.873	---	---	19	0.02	0.0096	0.0008	2.35	---	19	0.05	0.0164	0.0002	2.67	---	19	---	---	---	---	---					
39	0.0294	0.0090	3.82	---	---	39	0.47	0.0233	0.0070	3.34	---	39	0.58	0.0440	0.0004	3.73	---	39	---	---	---	---	---					
59	0.0369	0.0098	4.07	---	---	59	0.93	0.0309	0.0079	4.13	---	59	0.99	0.0315	0.0009	4.29	---	59	---	---	---	---	---					
79	0.0406	0.0103	4.73	---	---	79	1.39	0.0399	0.0081	4.79	---	79	1.46	0.0379	0.0074	5.14	---	79	---	---	---	---	---					
99	0.0466	0.0118	3.85	---	---	99	1.87	0.0474	0.0080	5.35	---	99	1.94	0.0477	0.0081	5.02	---	99	---	---	---	---	---					
119	0.0590	0.0148	3.65	---	---	119	2.34	0.0554	0.0097	5.75	---	119	2.42	0.0587	0.0089	5.90	---	119	---	---	---	---	---					
139	0.0598	0.0184	3.65	---	---	139	2.83	0.0644	0.0100	5.95	---	139	2.89	0.0598	0.0100	5.99	---	139	---	---	---	---	---					
159	0.0610	0.0130	3.86	---	---	159	3.31	0.0723	0.0100	6.05	---	159	3.38	0.0669	0.0112	5.96	---	159	---	---	---	---	---					
179	---	---	---	---	---	179	3.80	0.0807	0.0134	6.04	---	179	3.86	0.0736	0.0189	5.71	---	179	---	---	---	---	---					
Plan form C																												
0	-0.77	0.0010	0.0009	-0.11	0.0080	-0.0011	0	-0.80	0.0049	0.0072	-0.68	0.0047	-0.0048	0	-0.88	0.0037	0.0064	-0.57	0.0074	-0.0038	0	-1.12	0.0044	0.0072	-0.61	---	-0.0046	
19	0.0090	0.0087	1.03	0.0050	0.0089	---	19	0.32	0.0042	0.0070	1.29	0.0029	0.0046	19	0.41	0.0058	0.0069	0.83	0.0068	0.0078	---	19	0.60	0.0080	0.0072	1.89	---	0.0019
39	0.0158	0.0087	2.16	0.0143	0.0189	---	39	0.65	0.0136	0.0071	1.87	0.0105	0.0133	39	0.65	0.0133	0.0068	2.15	0.0084	0.0133	---	39	0.59	0.0091	0.0072	1.87	---	0.0091
59	0.0204	0.0098	3.09	0.0280	0.0289	---	59	0.95	0.0221	0.0072	3.00	0.0182	0.0220	59	0.93	0.0222	0.0075	3.41	0.0164	0.0222	---	59	0.96	0.0168	0.0072	2.85	---	0.0163
79	0.0279	0.0097	3.90	0.0302	0.0321	---	79	1.24	0.0311	0.0077	4.09	0.0255	0.0310	79	1.00	0.0311	0.0068	4.29	0.0244	0.0312	---	79	1.06	0.0244	0.0075	3.07	---	0.0255
99	0.0321	0.0104	4.74	0.0400	0.0494	---	99	1.63	0.0399	0.0083	4.81	0.0333	0.0401	99	1.46	0.0391	0.0073	5.35	0.0344	0.0393	---	99	1.46	0.0393	0.0079	3.83	---	0.0307
119	0.0361	0.0118	5.25	0.0490	0.0605	---	119	2.02	0.0490	0.0081	5.40	0.0403	0.0492	119	1.96	0.0477	0.0081	5.95	0.0493	0.0479	---	119	2.02	0.0479	0.0083	4.30	---	0.0378
139	0.0399	0.0123	5.75	0.0581	0.0714	---	139	2.43	0.0578	0.0088	5.87	0.0483	0.0582	139	2.44	0.0584	0.0089	6.24	0.0577	0.0577	---	139	2.46	0.0580	0.0080	4.95	---	0.0450
159	0.0438	0.0130	6.08	0.0675	0.0828	---	159	2.83	0.0670	0.0110	6.07	0.0563	0.0679	159	2.82	0.0684	0.0099	6.39	0.0587	0.0636	---	159	3.08	0.0610	0.0087	5.25	---	0.0515
179	0.0480	0.0139	6.27	0.0772	0.0947	---	179	3.24	0.0756	0.0180	6.27	0.0635	0.0768	179	3.24	0.0762	0.0111	6.31	0.0588	0.0768	---	179	3.61	0.0582	0.0097	5.39	---	0.0587
199	0.0521	0.0147	6.38	0.0867	0.1062	---	199	3.65	0.0835	0.0136	6.18	0.0698	0.0843	199	3.68	0.0779	0.0129	6.24	0.0592	0.0786	---	199	4.14	0.0645	0.0118	5.46	---	0.0628
30	0.0539	0.0086	4.6	0.0083	0.0030	30	0.87	0.0081	0.0071	1.05	0.0011	0.0001	30	0.87	0.0033	0.0066	0.50	0.0088	0.0038	30	1.12	0.0085	0.0070	0.36	---	0.0084		
45	0.0129	0.0089	1.45	0.0097	0.0189	---	45	0.61	0.0110	0.0069	1.18	0.0099	0.0061	45	0.60	0.0110	0.0066	1.67	0.0044	0.0109	---	45	0.61	0.0091	0.0069	1.31	---	0.0090
60	0.0204	0.0091	2.46	0.0174	0.0284	---	60	0.93	0.0167	0.0070	2.35	0.0130	0.0167	60	0.95	0.0190	0.0067	2.84	0.0115	0.0190	---	60	0.99	0.0168	0.0070	2.35	---	0.0104
75	0.0282	0.0094	3.42	0.0283	0.0383	---	75	1.24	0.0233	0.0073	3.44	0.0204	0.0233	75	1.24	0.0233	0.0070	3.84	0.0189	0.0233	---	75	1.44	0.0230	0.0073	3.16	---	0.0230
90	0.0361	0.0099	4.30	0.0382	0.0489	---	90	1.63	0.0329	0.0079	4.30	0.0276	0.0360	90	1.60	0.0353	0.0074	4.74	0.0261	0.0354	---	90	1.97	0.0302	0.0077	3.02	---	0.0304
105	0.0438	0.0106	5.03	0.0489	0.0597	---	105	2.02	0.0427	0.0084	5.06	0.0354	0.0429	105	1.96	0.0433	0.0080	5.43	0.0389	0.0433	---	105	2.46	0.0368	0.0082	2.47	---	0.0370
120	0.0517	0.0116	5.59	0.0585	0.0693	---	120	2.43	0.0515	0.0092	5.58	0.0429	0.0518	120	2.42	0.0507	0.0087	5.86	0.0395	0.0510	---	120	2.82	0.0439	0.0088	2.97	---	0.0442
135	0.0590	0.0126	5.94	0.0677	0.0795	---	135	2.83	0.0604	0.0101	6.00	0.0504	0.0608	135	2.82	0.0581	0.0095	6.10	0.0462	0.0583	---	135	3.26	0.0505	0.0096	2.86	---	0.0509
150	0.0669	0.0131	6.13	0.0701	0.0828	---	150	3.24	0.0694	0.0112	6.22	0.0581	0.0699	150	3.22	0.0698	0.0106	6.22	0.0492	0.0698	---	150	3.68	0.0570	0.0109	2.89	---	0.0576
165	0.0750	0.0139	6.15	0.0788	0.0950	---	165	3.65	0.0782	0.0124	6.38	0.0656	0.0788	165	3.61	0.0735	0.0118	6.25	0.0599	0.0780	---	165	4.14	0.0643	0.0121	2.93	---	0.0649
180	0.0831	0.0149	6.13	0.0872	0.1080	---	180	4.06	0.0869	0.0136	6.29	0.0730	0.0876	180	4.09	0.0808	0.0132	6.14	0.0599	0.0805	---	180	4.14	0.0714	0.0134	2.92	---	0.0723
30	0.0075	0.0079	0.97	0.0099	0.0075	30	0.88	0.0073	0.0073	1.00	0.0037	0.0078	30	0.88	0.0073	0.0073	1.00	0.0037	0.0078	30	1.13	0.0073	0.0093	0.81	---	0.0073		
45	0.0129	0.0089	1.45	0.0097	0.0189	---	45	0.61	0.0110	0.0069	1.18	0.0099	0.0061	45	0.60	0.0110	0.0066	1.67	0.0044	0.0109	---	45	0.61	0.0091	0.0069	1.31	---	0.0090
60	0.0204	0.0091	2.46	0.0174	0.0284	---	60	0.93	0.0167	0.0070	2.35	0.0130	0.0167	60	0.95	0.0190	0.0067	2.84	0.0115	0.0190	---	60	0.99	0.0168	0.0070	2.35	---	0.0104
75	0.0282	0.0094	3.42	0.0283	0.0383	---	75	1.24	0.0233	0.0073	3.44	0.0204	0.0233	75	1.24	0.0233	0.0070	3.84	0.0189	0.0233	---	75	1.44	0.0230	0.0073	3.16	---	0.0230
90	0.0361	0.0099	4.30	0.0382	0.0489	---	90	1.63	0.0329	0.0079	4.30	0.0276	0.0360	90	1.60	0.0353	0.0074	4.74	0.0261	0.0354	---	90	1.97	0.0302	0.0077	3.02	---	0.0304
105	0.0438	0.0106	5.03	0.0489	0.0597	---	105	2.02	0.0427	0.0084	5.06	0.0354	0.0429	105	1.96	0.0433	0.0080	5.43	0.0389	0.0433	---	105	2.46	0.0368	0.0082	2.47	---	0.0370
120	0.0517	0.0116	5.59	0.0585	0.0693	---	120	2.43	0.0515	0.0092	5.58	0.0429	0.0518	120	2.42	0.0507	0.0087	5.86	0.0395	0.0510	---	120	2.82	0.0439	0.0088	2.97	---	0.0442
135	0.0590	0.0126	5.94	0.0677	0.0795	---	135	2.83	0.0604	0.0101	6.00	0.0504	0.0608	135	2.82	0.0581	0.0095	6.10	0.0462	0.0583	---	135	3.26	0.0505	0.0096	2.86	---	0.0509
150	0.0669	0.0131	6.13	0.0701	0.0828	---	150	3.24	0.0694	0.0112	6.22	0.0581	0.0699	150	3.22	0.0698	0.0106	6.22	0.0492	0.0698	---	150	3.68	0.0570	0.0109	2.89	---	0.0576
165	0.0750	0.0139	6.15	0.0788	0.0950	---	165	3.65	0.0782	0.0124	6.38	0.0656	0.0788	165	3.61	0.0735	0.0118	6.25	0.0599	0.0780	---	165	4.14	0.0643	0.0121	2.93	---	0.0649
180	0.0831	0.0149	6.13	0.0872	0.1080	---	180	4.06	0.0869	0.0136	6.29	0.0730	0.0876	180	4.09	0.0808	0.0132	6.14	0.0599	0.0805	---	180	4.14	0.0714	0.0134	2.92	---	0.0723
30	0.0075	0.0079	0.97	0.0099	0.0075	30	0.88	0.007																				

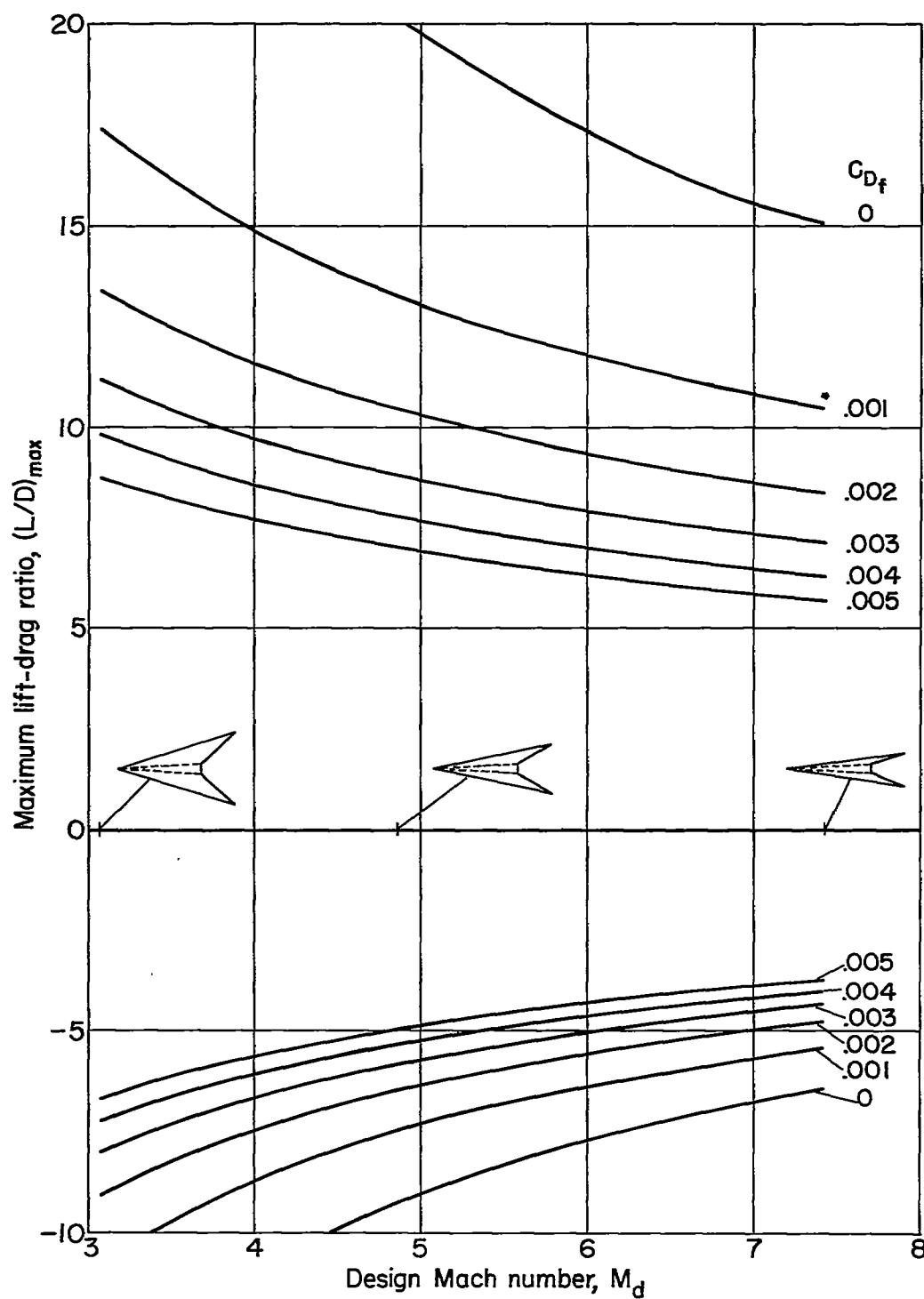


Figure 1.- Maximum lift-drag ratios predicted for flat-top configurations with 5° semivertex angle half-cone bodies.

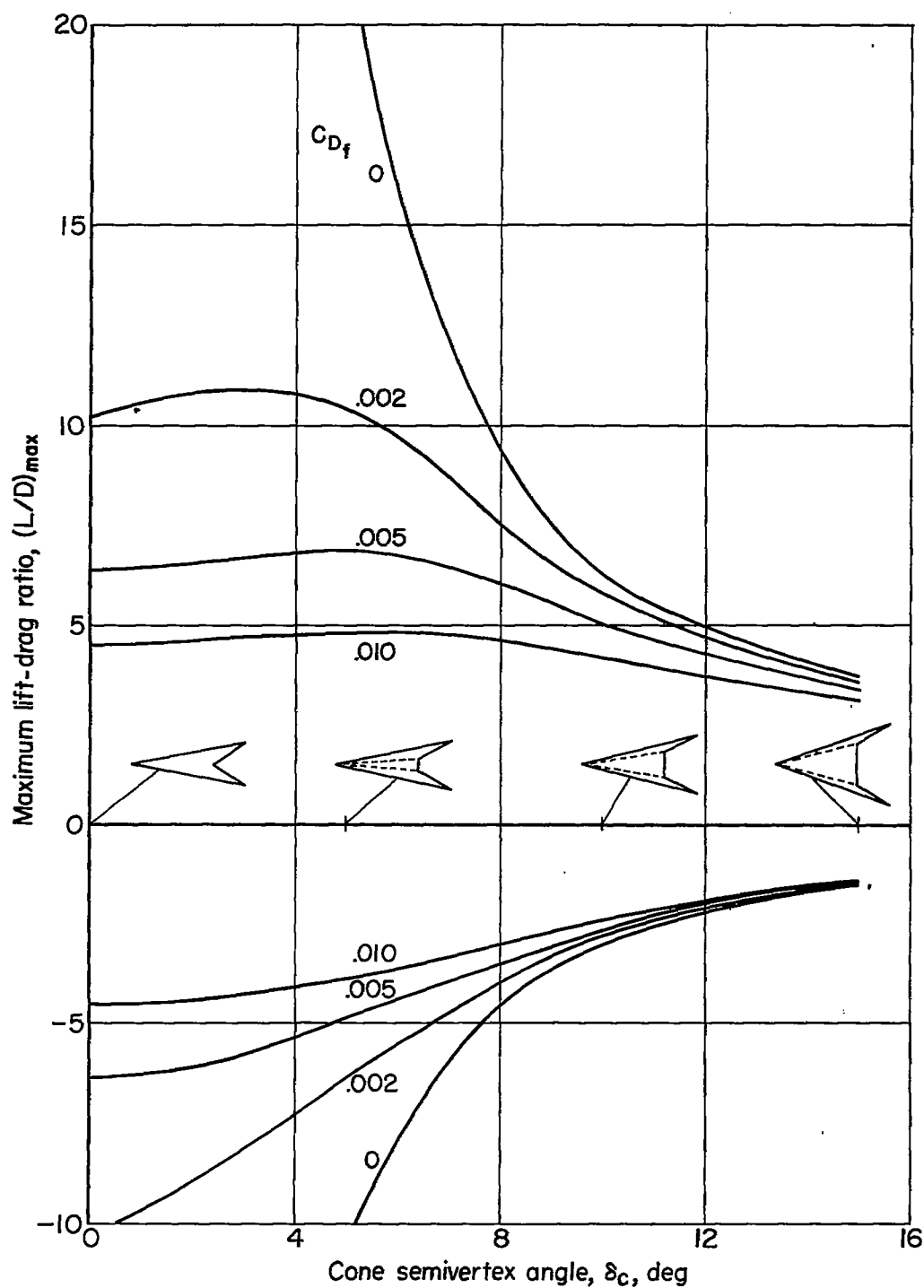
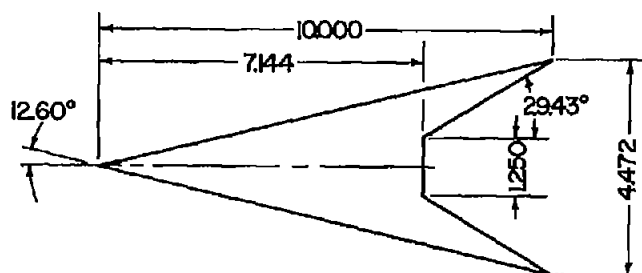
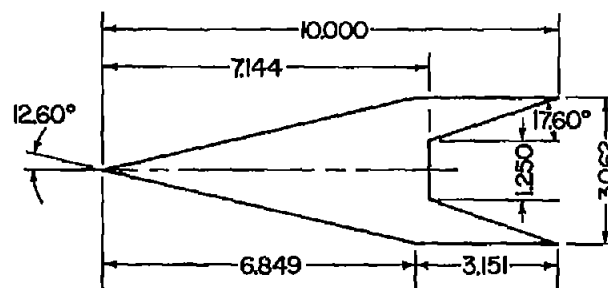


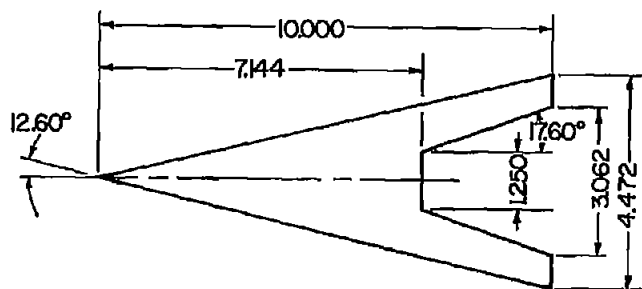
Figure 2.- Effect of variations in cone semivertex angle on predicted maximum lift-drag ratios of conical flat-top configurations ($M_\infty = 5$).



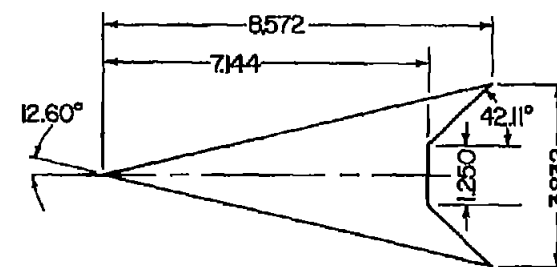
Plan form A



Plan form B

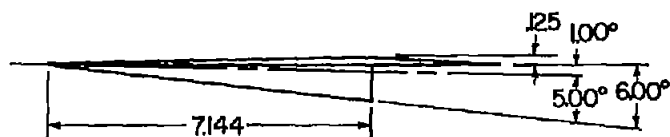


Plan form C

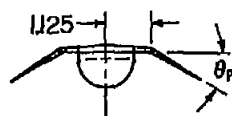


Plan form D

Note: All dimensions in inches.



Side view



Front view

Plan form	A	B	C	D
Aspect ratio	1.41	.67	1.23	1.15
Wing area, S	14.19	13.98	16.20	12.79
Flap area, S_F	3.33	—	4.99	—
Flap area/wing area, S_F/S	.24	—	.31	—

Figure 3.- Test models.

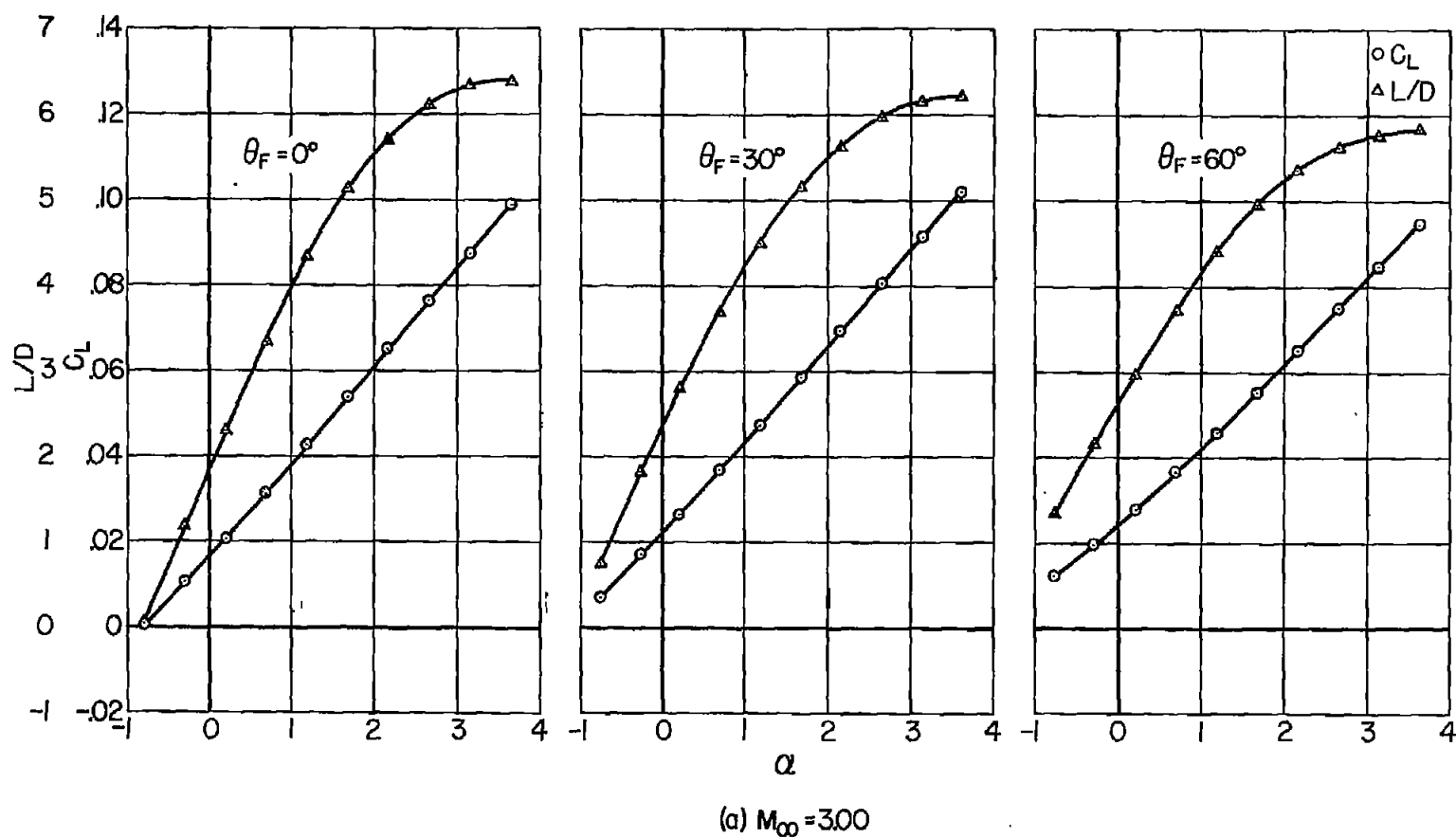
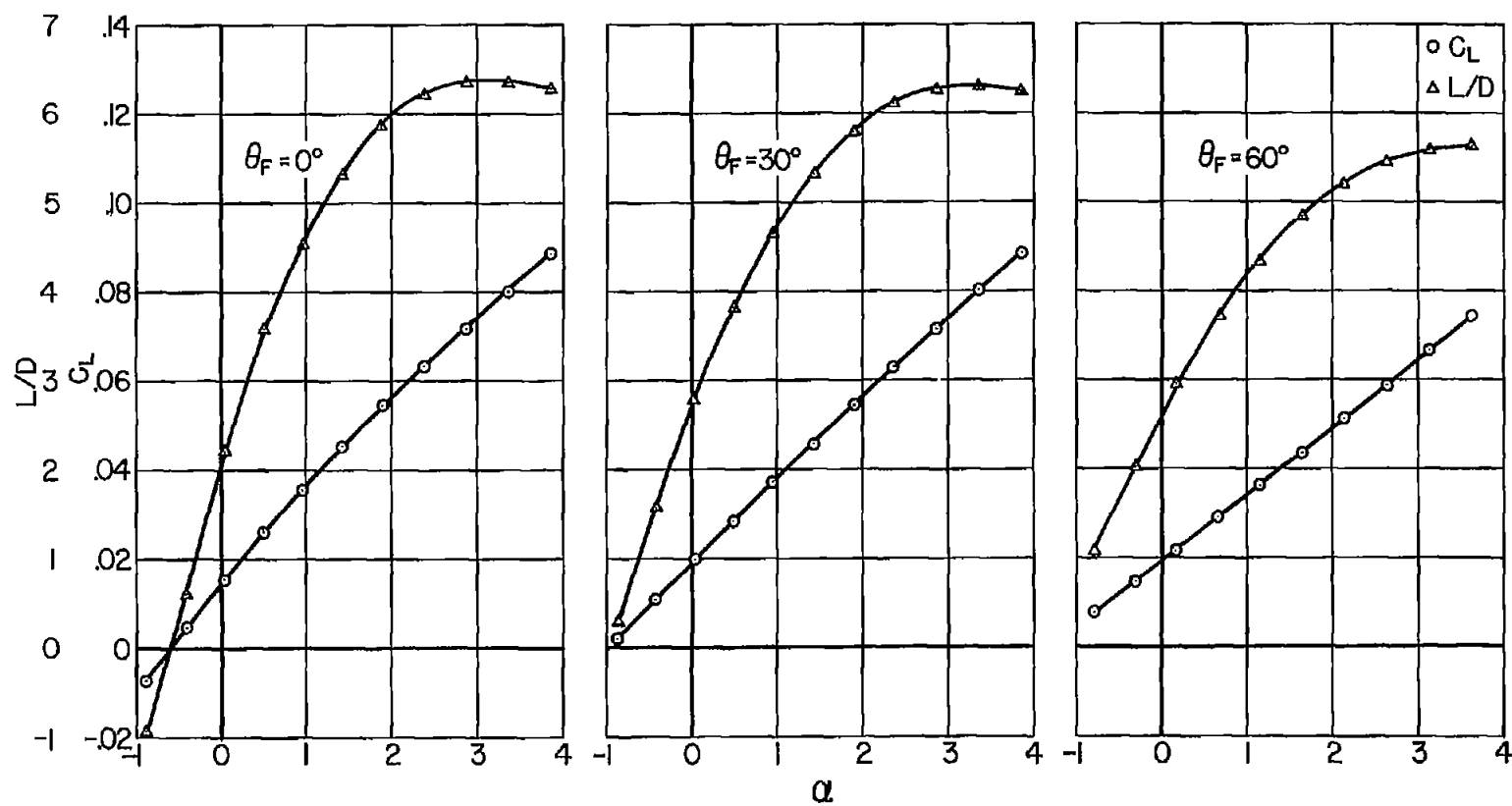


Figure 4.- Lift coefficients and lift-drag ratios obtained experimentally with flat-top model employing plan form A.



(b) $M_\infty = 4.24$

Figure 4.- Continued.

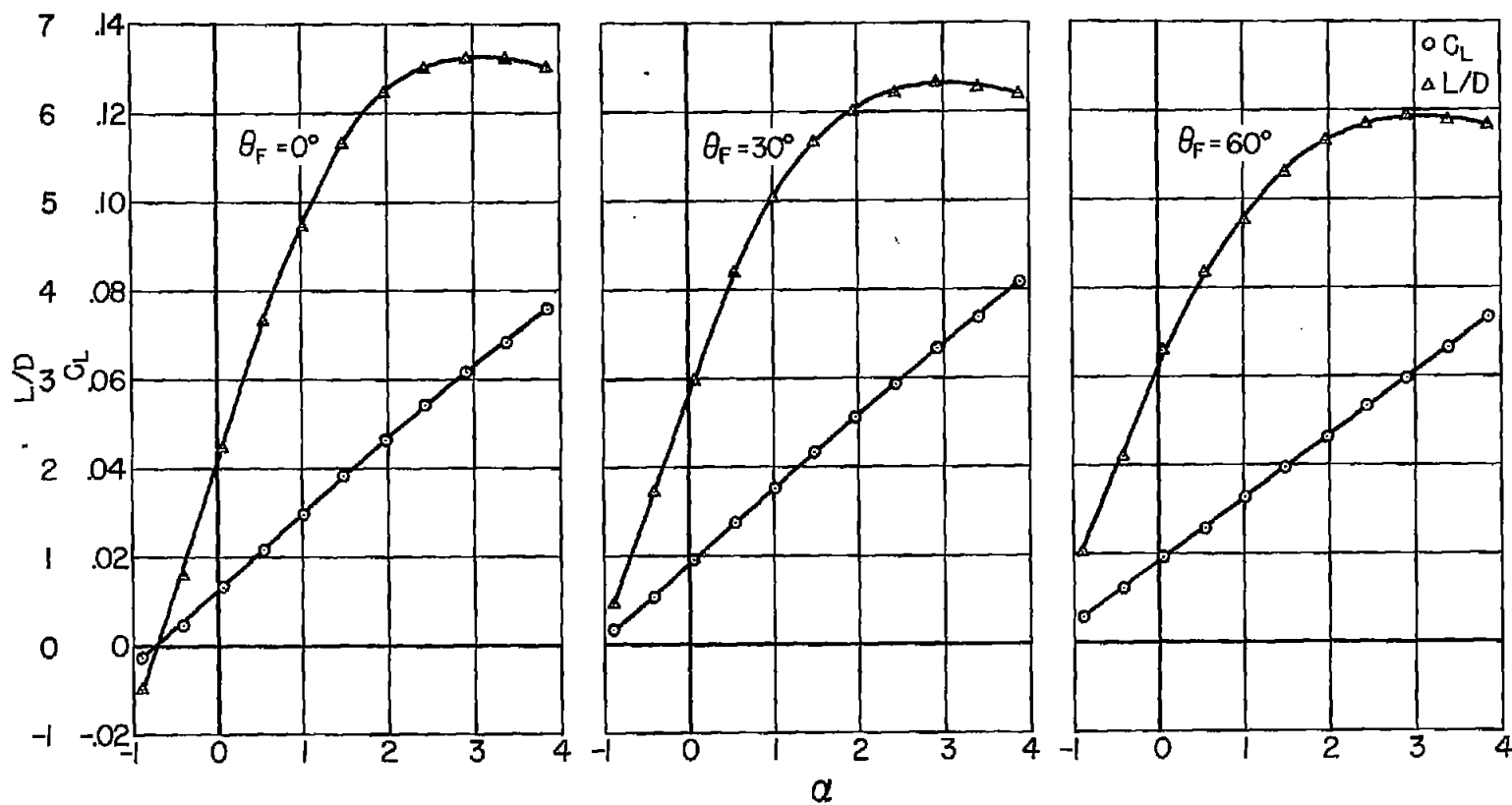
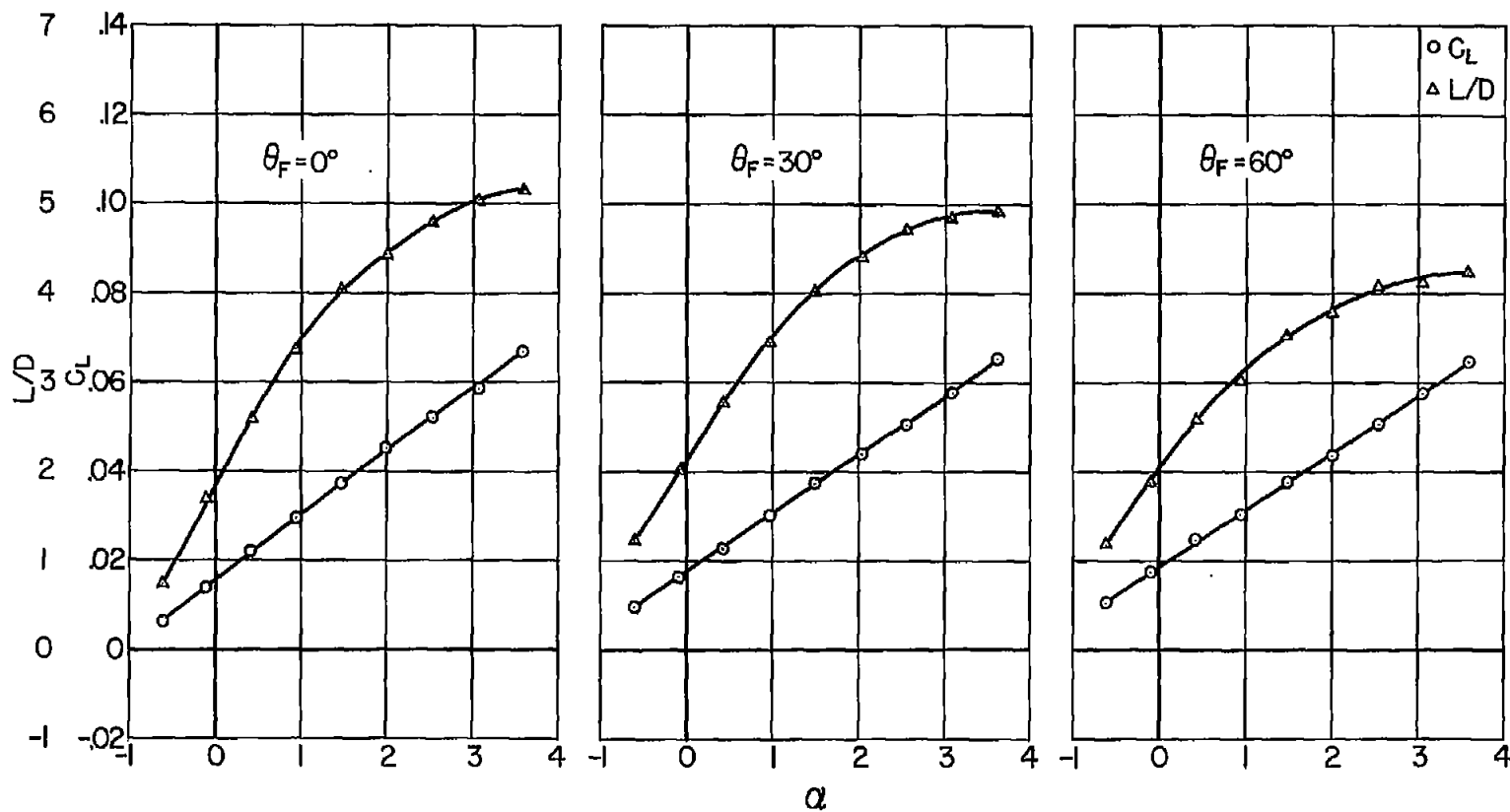
(c) $M_\infty = 5.05$

Figure 4.- Continued.



(d) $M_\infty = 6.28$

Figure 4.- Concluded.

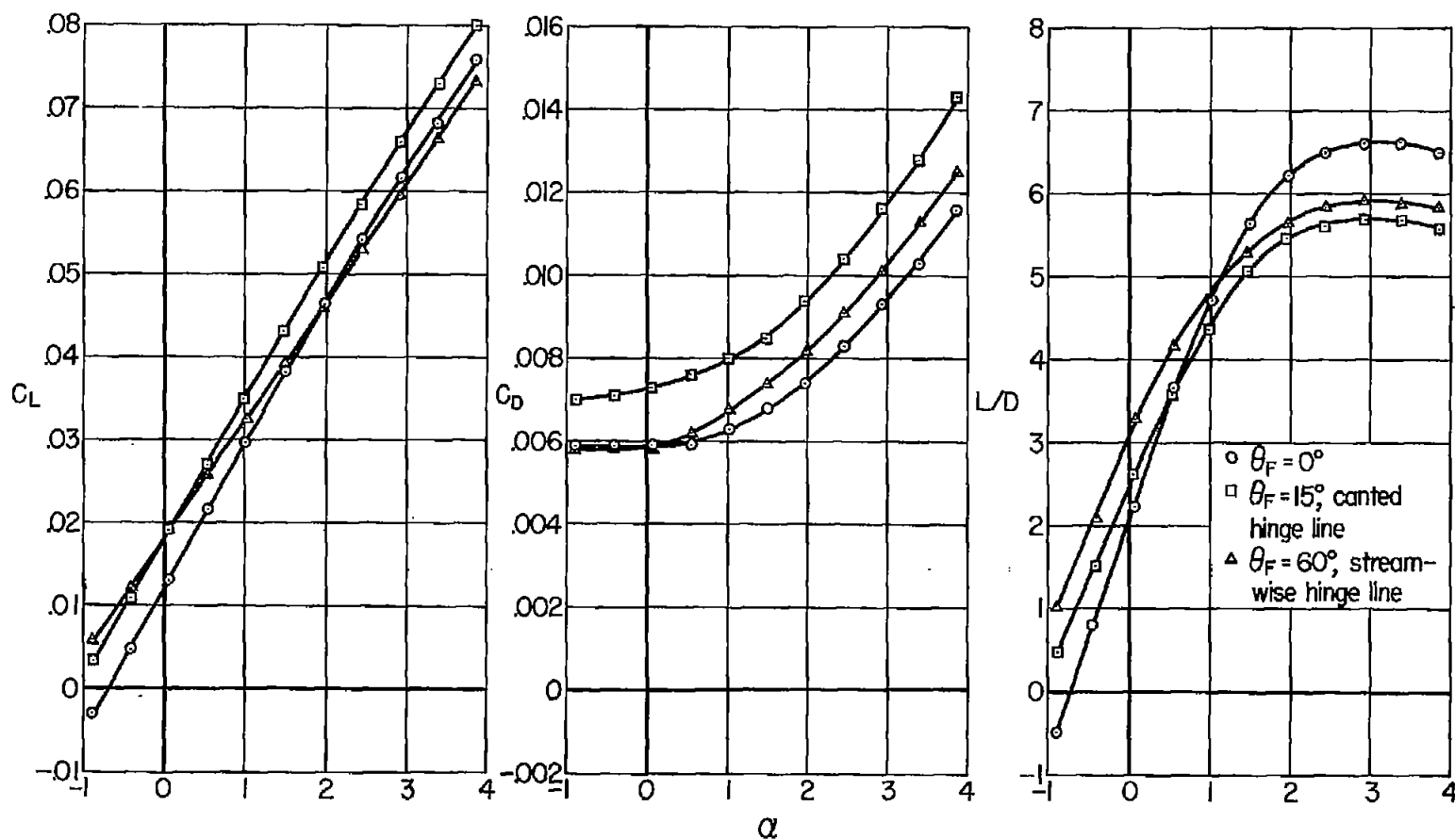


Figure 5.- Effect of various flap arrangements on the lift and drag characteristics of flat-top model employing plan form A ($M_\infty = 5.05$).

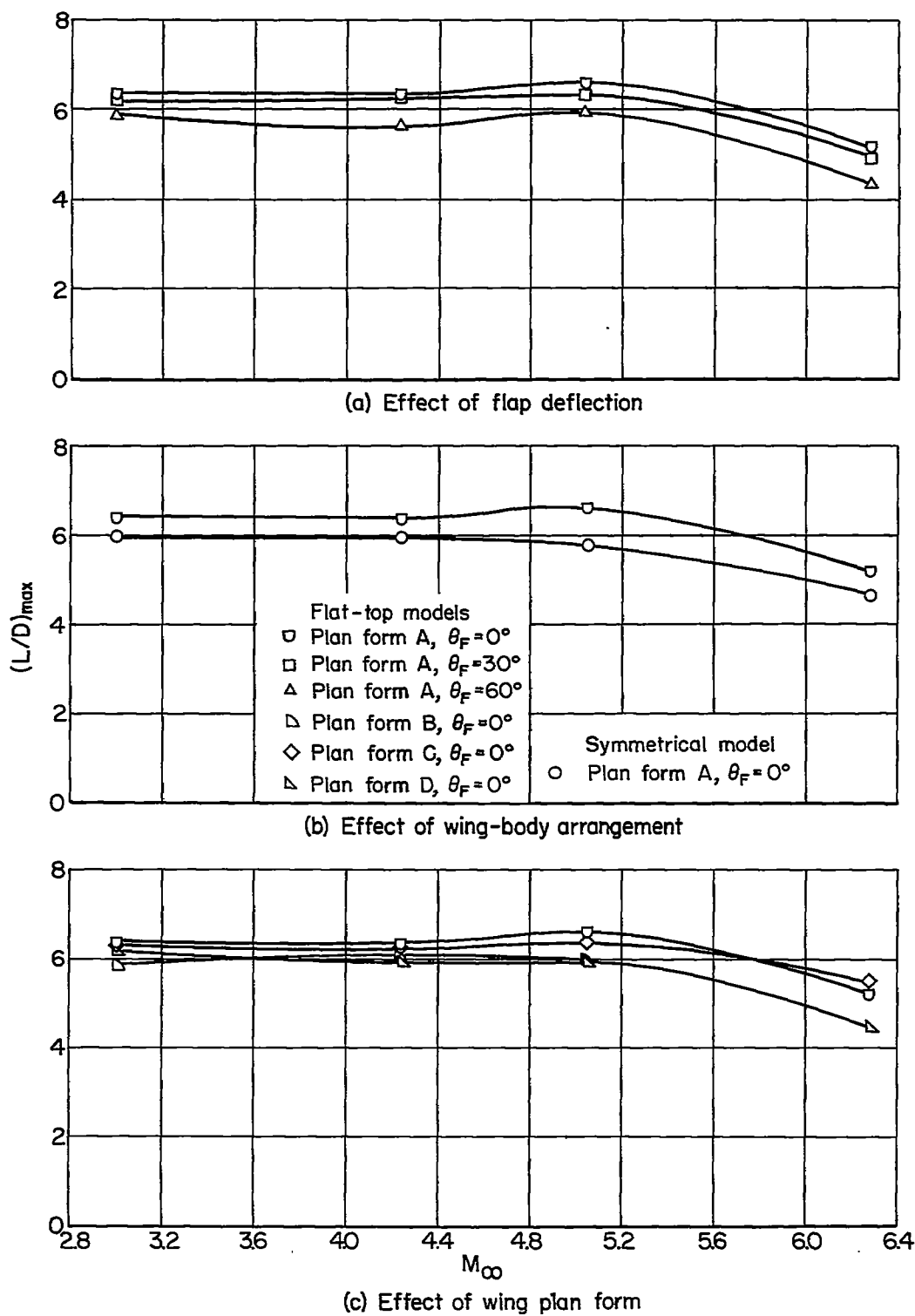


Figure 6.- Variation of maximum lift-drag ratios with Mach number.

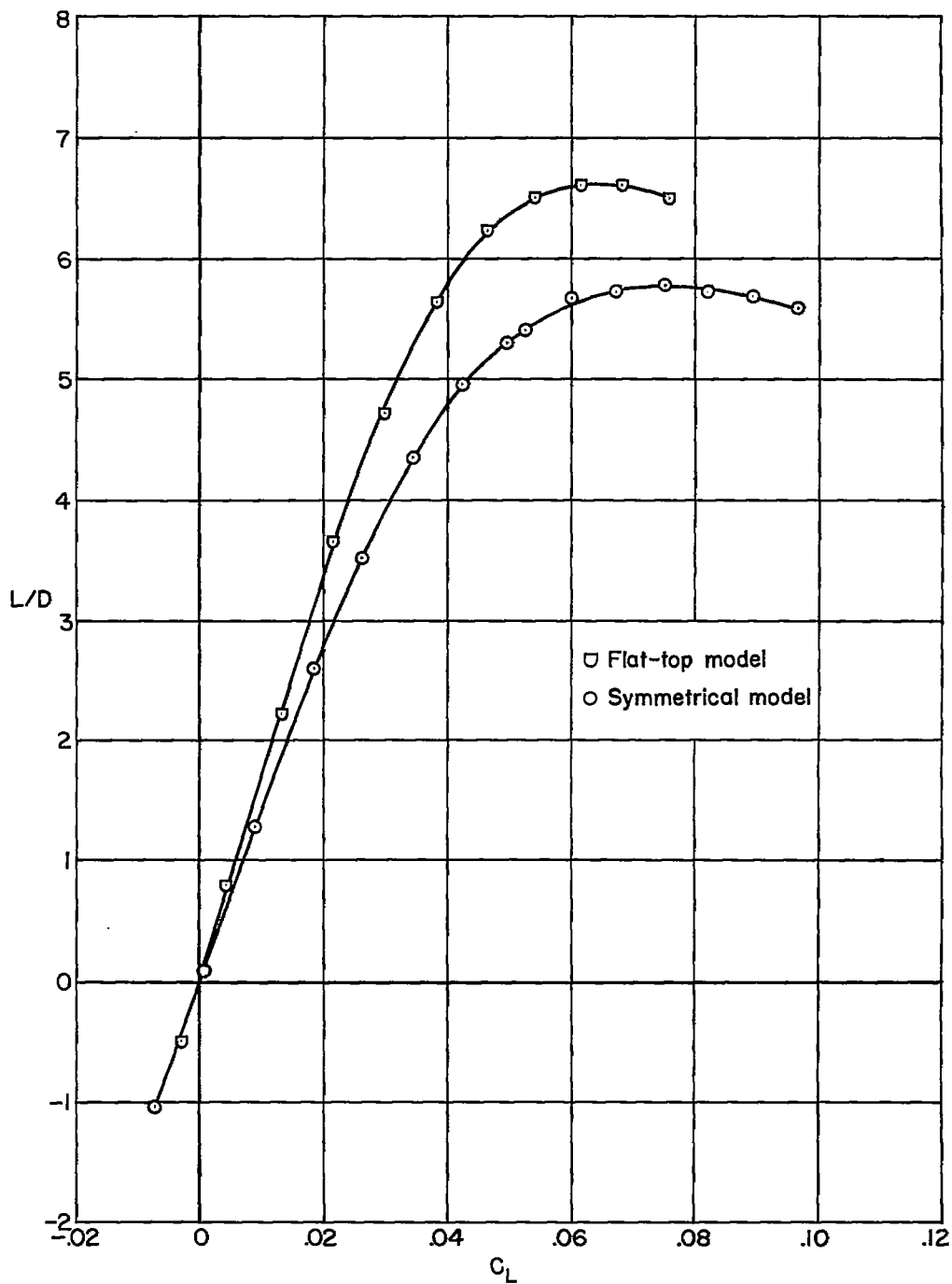


Figure 7.- Comparison of lift-drag ratios obtained with flat-top model and with symmetrical model, both employing plan form A ($M_\infty = 5.05$, $\theta_F = 0^\circ$).

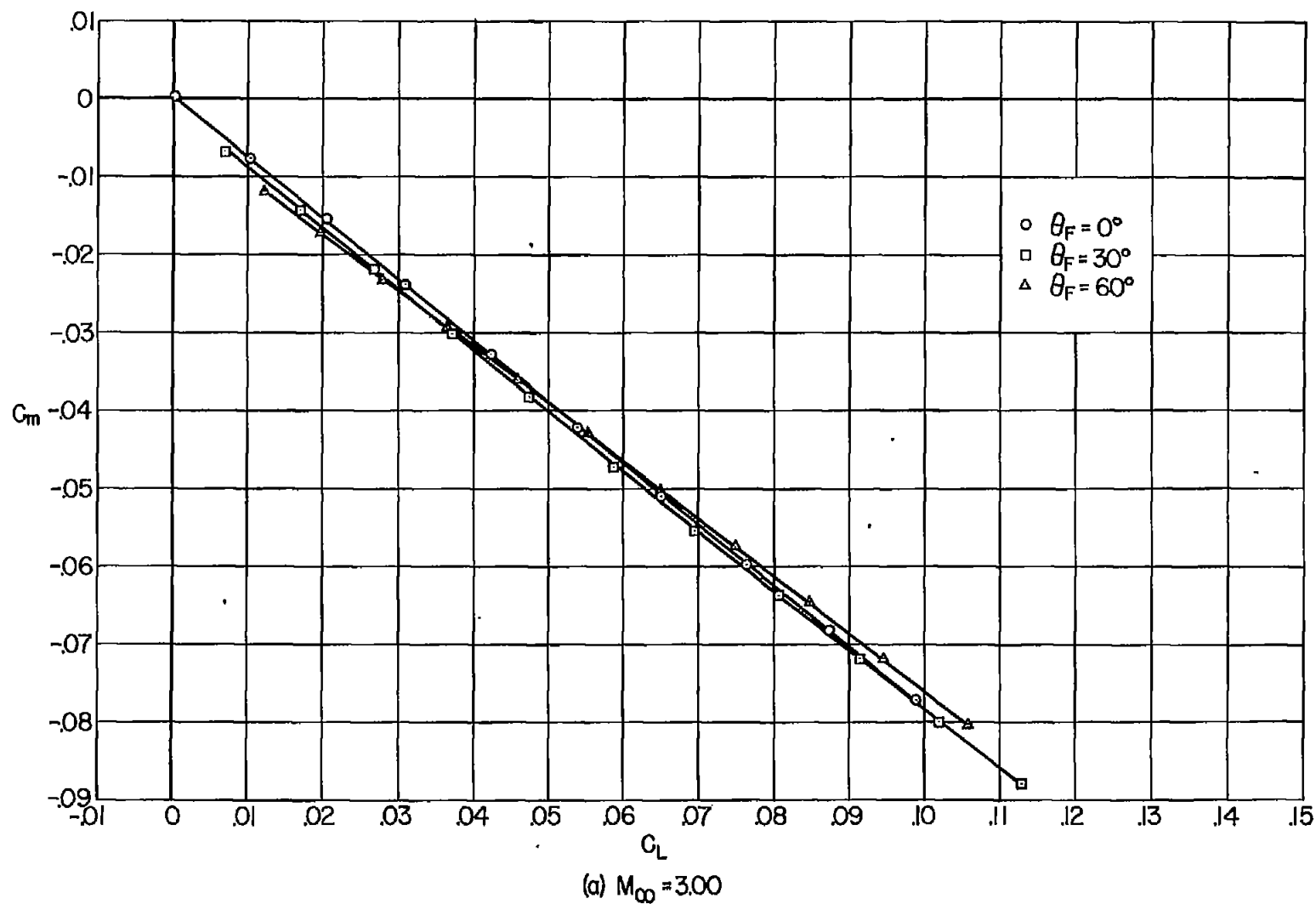
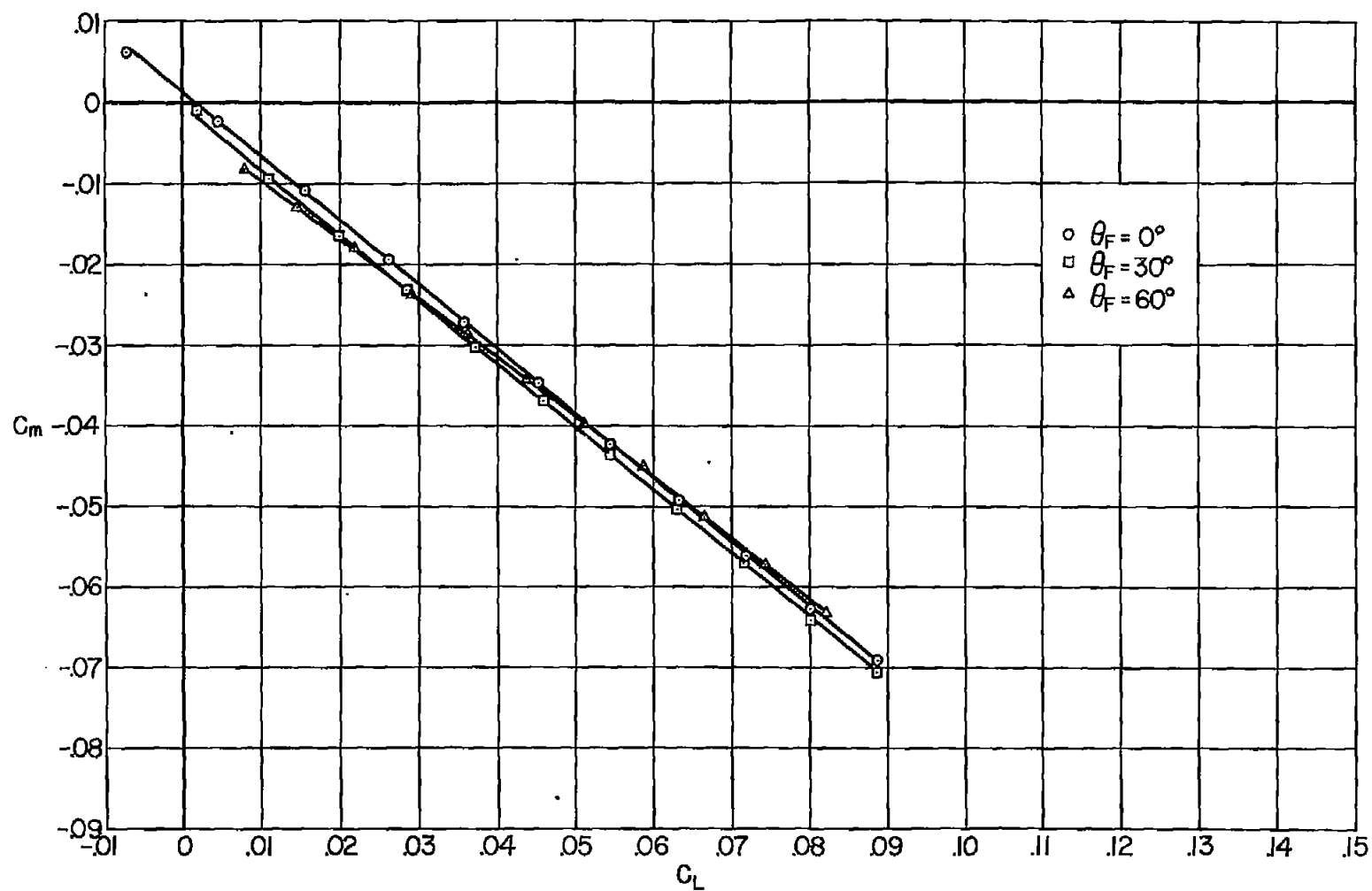
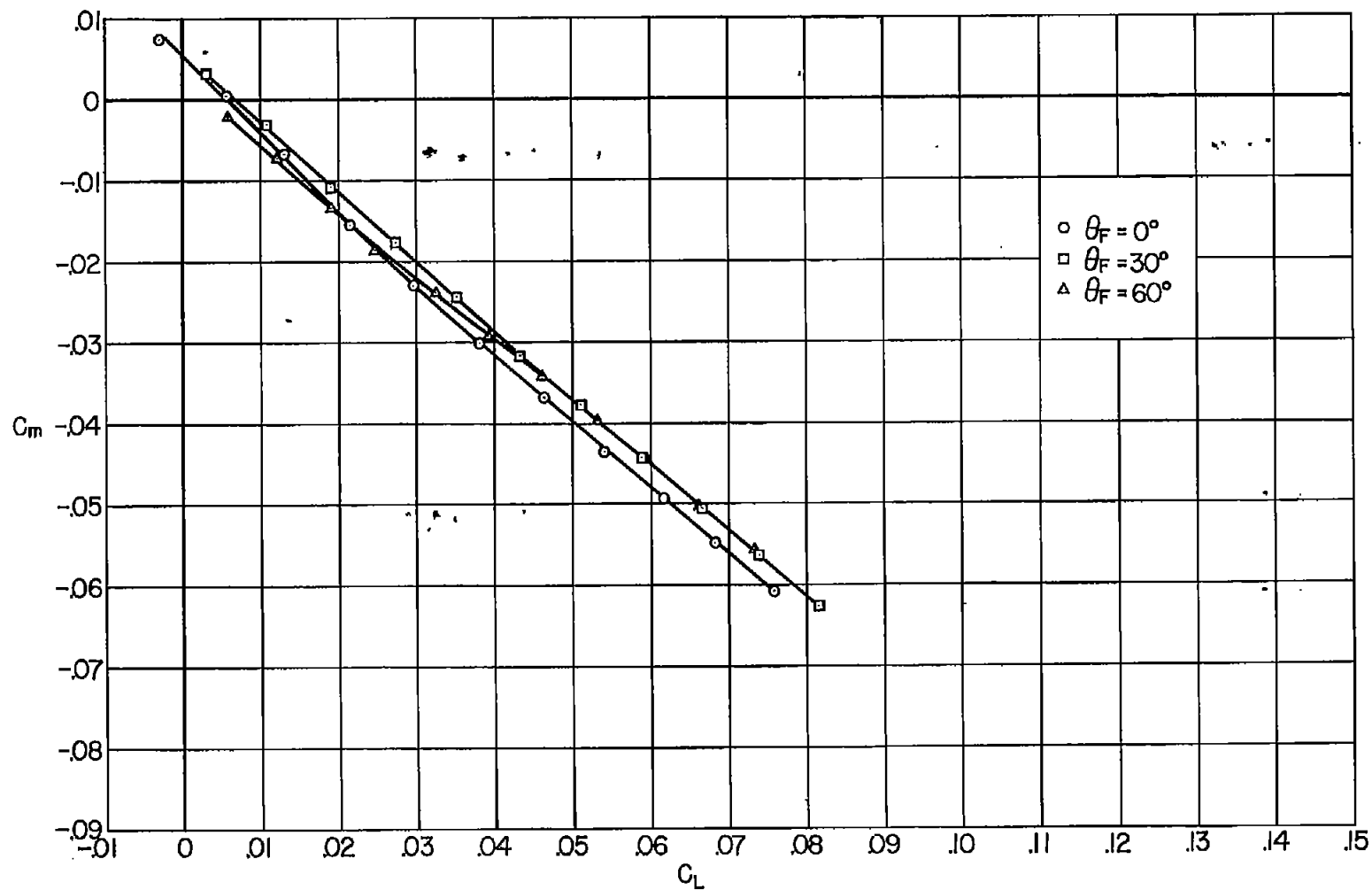


Figure 8.- Static longitudinal stability characteristics of flat-top model employing plan form A.



(b) $M_\infty = 4.24$

Figure 8.- Continued.



(c) $M_\infty = 5.05$

Figure 8.- Concluded.

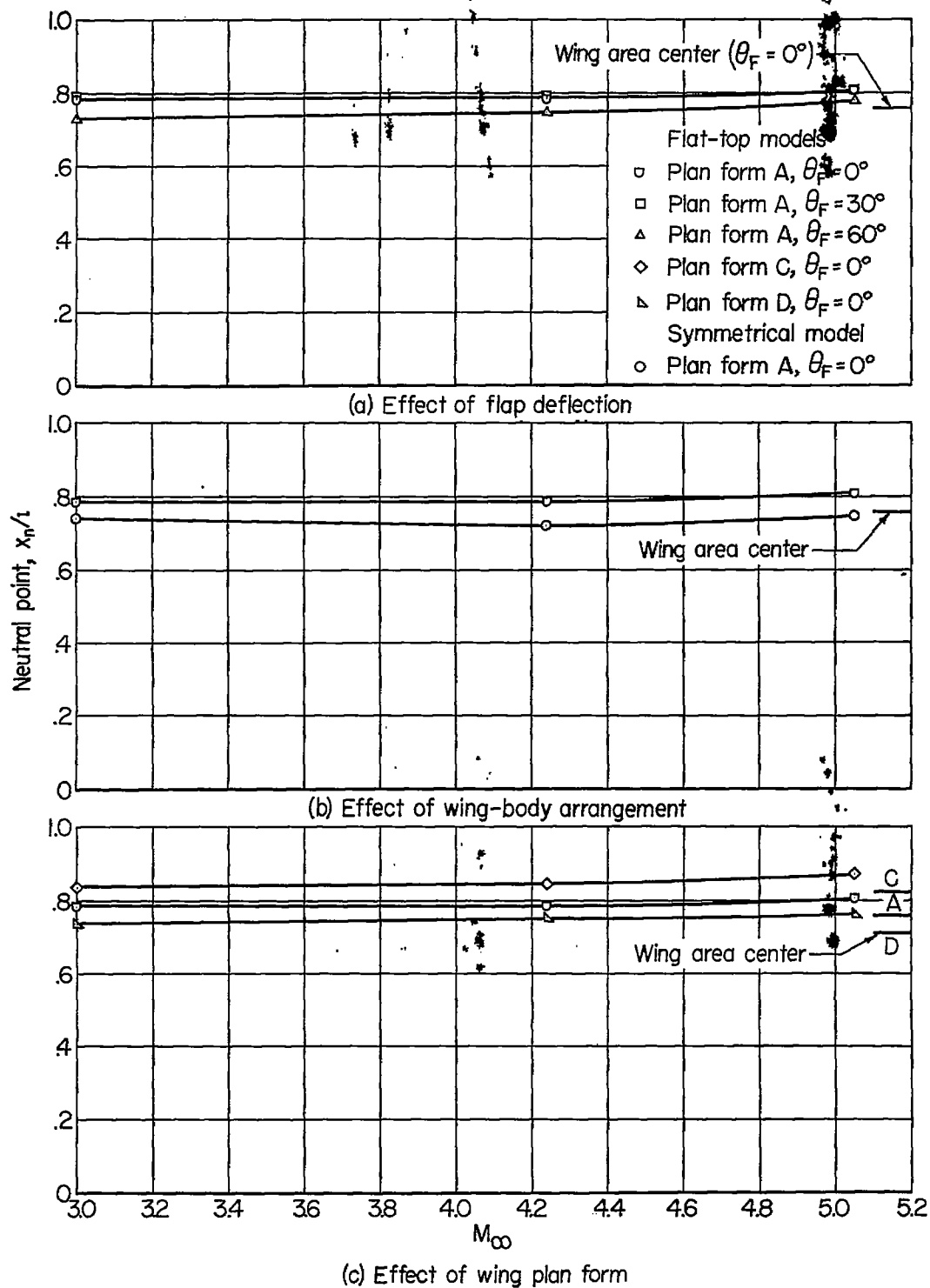


Figure 9.- Variation of neutral points with Mach number.